

1 **AKT1-FOXO4 AXIS RECIPROCALLY REGULATES HEMOCHORIAL**
2 **PLACENTATION**

3

4 **Keisuke Kozai^{1,*§}, Ayelen Moreno-Irusta^{1*,¥}, Khursheed Iqbal¹, Mae-Lan Winchester^{2†},**
5 **Regan L. Scott¹, Mikaela E. Simon¹, Masanaga Muto^{1‡}, Marc R. Parrish², and Michael**
6 **J. Soares^{1,2,3,¥}**

7

8 **¹Institute for Reproduction and Developmental Sciences, Department of Pathology &**
9 **Laboratory Medicine, University of Kansas Medical Center, Kansas City, KS**

10

11 **²Department of Obstetrics and Gynecology, University of Kansas Medical Center,**
12 **Kansas City, KS**

13

14 **³Center for Perinatal Research, Children's Mercy Research Institute, Children's Mercy,**
15 **Kansas City, MO**

16

17 ***Contributed equally**

18 **¥Correspondence: amoreno2@kumc.edu or msoares@kumc.edu**

19

20 **§Present address:** Department of Obstetrics and Gynecology, University of Missouri-Kansas
21 **City School of Medicine, Kansas City, MO**

22

23 **†Present address:** Department of Obstetrics and Gynecology, University Hospital, Case
24 **Western Reserve University, Beachwood, OH 44122**

25

26 **‡Present address:** Department of Stem Cells and Human Disease Models, Research Center
27 **for Animal Life Science, Shiga University of Medical Science, Seta, Tsukinowa-cho, Otsu,**
28 **Shiga 520-2192, Japan**

29

30 **Running title: AKT1 and uteroplacental development**

31

32 **Keywords: AKT1, FOXO4, trophoblast, placenta, pregnancy, rat, genome editing**

33 **SUMMARY STATEMENT**

34 Genome-edited rat models were utilized to investigate roles for AKT1 and FOXO4 in
35 hemochorial placentation. AKT1 and FOXO4 possess reciprocal actions in regulating
36 development of the hemochorial placenta.

37

38 **ABSTRACT**

39 Hemochorial placentation involves the differentiation of specialized cells called invasive
40 trophoblast cells possessing the capacity to exit the placenta and invade into the uterus where
41 they restructure the vasculature. Invasive trophoblast cells arise from a well-defined
42 compartment within the placenta, referred to as the junctional zone in the rat and the
43 extravillous trophoblast cell column in the human. In this study, we investigated roles for
44 AKT1, a serine/threonine kinase, in placental development using a
45 genome-edited/loss-of-function rat model. Disruption of AKT1 resulted in placental, fetal,
46 and postnatal growth restriction. Forkhead box O4 (*Foxo4*), which encodes a transcription
47 factor and known AKT substrate, was abundantly expressed in the junctional zone and
48 invasive trophoblast cells of the rat placentation site. *Foxo4* gene disruption using
49 genome-editing resulted in placentomegaly, including an enlarged junctional zone. AKT1 and
50 FOXO4 regulate the expression of many of the same transcripts expressed by trophoblast
51 cells; however, in opposite directions. In summary, we have identified AKT1 and FOXO4 as
52 part of a regulatory network that reciprocally controls critical indices of hemochorial placenta
53 development.

54

55 **INTRODUCTION**

56 The placenta is an extraembryonic structure essential for normal fetal development
57 (**Maltepe & Fisher, 2015; Burton *et al.*, 2016**). Placentas possess two main functions: i)
58 transformation of the maternal environment to support viviparity and ii) regulation of the
59 transfer of nutrients to the fetus (**Gardner & Beddington, 1988; Soares *et al.*, 2018; Knöfler
60 *et al.*, 2019**). These specialized functions are ascribed to trophoblast cells, which differentiate
61 along a multi-lineage pathway and are situated within specific compartments of the placenta
62 (**Gardner & Beddington, 1988; Soares *et al.*, 2018; Knöfler *et al.*, 2019; Aplin & Jones,
63 2021**). Placentas come in different shapes, sizes, and connectivity to the mother (**Wooding &
64 Burton, 2008; Roberts *et al.*, 2016**). Placentation in some mammalian species is
65 characterized by trophoblast cells migrating into the maternal uterus where they modify the
66 vasculature facilitating maternal nutrient flow to the placenta (**Pijnenborg *et al.*, 1981;
67 Soares *et al.*, 2018**). This type of placenta is referred to as hemochorial (**Wooding & Burton,
68 2008; Roberts *et al.*, 2016**). The human and rat possess hemochorial placentation where
69 invasive trophoblast cells migrate deep into the uterine parenchyma (**Pijnenborg *et al.*, 1981;
70 Soares *et al.*, 2018**). Regulation of deep hemochorial placentation is poorly understood. The
71 rat represents a useful animal model for investigating the regulation of deep hemochorial
72 placentation (**Pijnenborg & Vercruyssen, 2010; Soares *et al.*, 2012; Shukla & Soares,
73 2022**).

74

75 The rat placenta can be divided into two main compartments: i) junctional zone; ii)
76 labyrinth zone (**Ain *et al.*, 2006; Soares *et al.*, 2012**). The junctional zone compartment of
77 the placenta is situated proximal to the uterine endometrium and is responsible for
78 transforming the maternal environment, whereas the labyrinth zone is located between the
79 junctional zone and fetus where it facilitates nutrient delivery to the fetus (**Knipp *et al.*,**

80 **1999; Soares *et al.*, 2012**). Junctional zone-specific functions include the production of
81 peptide and steroid hormones that target maternal organs and the generation of invasive
82 trophoblast cells that migrate into and restructure the uterine parenchyma (**Soares *et al.*, 1996,**
83 **2012**). The extravillous trophoblast cell column is a structure within the human placentation
84 site, which shares some of these same responsibilities (**Soares *et al.*, 2018; Knöfler *et al.*,**
85 **2019**). The junctional zone and extravillous trophoblast cell column are pivotal to the
86 regulation of maternal adaptations to pregnancy, yet little is known about how they are
87 regulated.

88

89 In this report, we focus on the phosphatidylinositol 3-kinase (**PI3K**)/AKT pathway and its
90 involvement in regulating junctional zone biology. AKT1 is one of three AKT
91 serine/threonine kinases and represents an integral component of signal transduction
92 pathways regulating cell proliferation, differentiation, migration, survival, and metabolism
93 (**Manning & Toker, 2017; Cole *et al.*, 2019**). AKT1 has also been implicated in placentation
94 and trophoblast cell development through rodent mutagenesis experiments and investigations
95 with human trophoblast cells (**Kamei *et al.*, 2002; Yang *et al.*, 2003; Qiu *et al.*, 2004; Dash
96 *et al.*, 2005; Kent *et al.*, 2010, 2011, 2012; Plaks *et al.*, 2011; Haslinger *et al.*, 2013;
97 **Sharma *et al.*, 2016**). Disruptions in AKT signaling have been connected to trophoblast cell
98 dysfunction leading to recurrent pregnancy loss, preeclampsia, and infertility (**Pollheimer &
99 Knöfler, 2005; Ferretti *et al.*, 2007; Fisher, 2015; Burton & Jauniaux, 2018**). Herein we
100 show that AKT1 inactivation leads to placental and fetal growth restriction in the rat. AKT1
101 acts via phosphorylation of its target proteins leading to functional changes, including
102 activation or inhibition of target protein function (**Manning & Toker, 2017; Cole *et al.*,**
103 **2019**). We identified forkhead box O4 (**FOXO4**), a transcription factor, as an AKT1 substrate
104 within the rat junctional zone and in rat trophoblast cells and demonstrated FOXO4**

105 involvement in junctional zone development and the regulation of trophoblast cell
106 differentiation.

107

108 **RESULTS**

109 **Generation of an *Akt1* mutant rat model**

110 AKT1 and phosphorylated AKT are ubiquitously expressed throughout the rat
111 placentation site (**Fig. S1A**). We examined the role of AKT1 in regulating deep placentation
112 in the rat using CRISPR/Cas9 genome editing. A mutant rat strain possessing a 1,332 bp
113 deletion within the *Akt1* gene was generated (**Fig. 1A and B**). The deletion included part of
114 Exon 4, the entire region spanning Exon 5 through Exon 6, and part of Exon 7 and led to a
115 frameshift and premature stop codon (**Fig. 1A and B**). The deletion effectively removed the
116 kinase domain and regulatory regions of AKT1 (**Fig. 1C**). The *Akt1* mutation was
117 successfully transmitted through the germline. A rat colony possessing the *Akt1* mutation was
118 established and maintained via heterozygous x heterozygous breeding. Mating of
119 heterozygotes produced the predicted Mendelian ratio (**Fig. 1D; Table S1**). Placental tissues
120 possessing a homozygous deletion within the *Akt1* locus (*Akt1*^{-/-}) were deficient in AKT1
121 protein and exhibited prominent deficits in pan-AKT and phospho-AKT protein expression
122 (**Fig. 1E**). Residual AKT activity could have arisen from AKT2 or AKT3, as previously
123 demonstrated for rat trophoblast cells (**Kent et al., 2011**). These findings support the
124 successful disruption of the *Akt1* locus and are consistent with AKT1 being the predominant
125 AKT isoform within the placenta (**Yang et al., 2003; Kent et al., 2011; Haslinger et al.,**
126 **2013**).

127

128 **AKT1 deficiency results in placental, fetal, and postnatal growth restriction**

129 Disruption of the *Akt1* locus in the mouse disrupts placental, fetal, and postnatal growth

130 (Chen *et al.*, 2001; Cho *et al.*, 2001; Yang *et al.*, 2003; Plaks *et al.*, 2011; Kent *et al.*, 2012).

131 We observed a similar phenotype in the rat. Gestation day (gd) 18.5 placental and fetal
132 weights and postnatal pup weights were significantly smaller in the *Akt1*^{-/-} rat model when
133 compared to *Akt1*^{+/+} rats (Fig. 2A-H). Junctional and labyrinth zone compartments of the
134 placenta were also significantly smaller in *Akt1*^{-/-} placentas (Fig. 2D, E, I).

135

136 **AKT1 regulates junctional zone and invasive trophoblast cell phenotypes**

137 Transcript profiles were determined for *Akt1*^{+/+} and *Akt1*^{-/-} gd 18.5 junctional zone tissues
138 using RNA-sequencing (RNA-seq). The size and morphological phenotypes associated with
139 inactivation of AKT1 were associated with distinct transcript profiles (Fig. 3; Table S2).
140 Disruption of AKT1 resulted in upregulation of 254 transcripts and downregulation of 333
141 transcripts (Table S2). Pathway analysis included signatures for cell cycle, DNA replication,
142 cellular senescence, and PI3K-AKT signaling pathways (Fig. 3A, Table S3). Transcripts
143 encoding cell cycle progression were consistently repressed in the *Akt1*^{-/-} junctional zones
144 (Fig. 3A and B). In addition, we also observed prominent downregulation of a member of the
145 expanded prolactin (PRL) gene family, *Prl8a4* (2-fold), and the upregulation of cellular
146 communication network factor 3 (3-fold), *Ccn3*, also called *Nov*; Fig. 3B).

147

148 The junctional zone serves as the source of invasive trophoblast cells entering the uterus.
149 Consequently, we investigated the uterine-placental interface of *Akt1*^{+/+} and *Akt1*^{-/-} placentas
150 and monitored the surface area occupied by intrauterine invasive trophoblast cells and the
151 expression of invasive trophoblast cell-specific transcripts. *Akt1*^{-/-} invasive trophoblast cells
152 exhibited decreased infiltration into the uterus (Fig. 3C-E). The decrease in trophoblast
153 invasion was proportional to the size of *Akt1*^{+/+} versus *Akt1*^{-/-} junctional zone compartments
154 (Fig. S1B). We also observed approximately a 50% decrease in the expression of cytokeratin

155 transcripts, which are expressed by invasive trophoblast cells within the uterine-placental
156 interface (**Fig. 3F**).

157

158 Collectively, the data indicate that AKT1 signaling has profound effects on development
159 of the junctional zone and the invasive trophoblast cell lineage.

160

161 **FOXO4 is a target of PI3K/AKT signaling**

162 Forkhead box (**FOX**) transcription factors are known targets of PI3K/AKT signaling and
163 have key roles in regulating developmental processes (**Lam et al., 2013; Schmitt-Ney, 2020;**
164 **Herman et al., 2021**). We interrogated RNA-seq datasets from wild type gd 18.5 junctional
165 zone for FOX family transcription factors. Transcripts for several FOX transcription factors
166 were detected (transcripts per million, TPM value ≥ 1.0) (**Fig. 4A**). *Foxo4* transcripts were
167 striking in their abundance relative to all other FOX family members. AKT1 did not
168 significantly affect expression levels for any of the FOX family transcripts (**Table S2**). *Foxo4*
169 transcripts were specifically localized to the junctional zone and a subset of invasive
170 trophoblast cells (**Fig. 4B and C**). FOXO4 protein and phosphorylated FOXO4 exhibited
171 similar tissue distributions (**Fig. S2A**). Phosphorylated FOXO4 protein was significantly
172 diminished in *Akt1* null junctional zones (**Fig. 4D, Fig S2B**). We next explored FOXO4 in
173 differentiated rat trophoblast stem (**TS**) cells (**Asanoma et al., 2011**). Rat TS cells can
174 differentiate into trophoblast giant cells and spongiotrophoblast cells and represent an
175 effective in vitro model for investigating junctional zone development (**Chakraborty et al.,**
176 **2011, 2016; Asanoma et al., 2012; Kubota et al., 2015; Muto et al., 2021; Varberg et al.,**
177 **2021**). *Foxo4* transcript and total and phosphorylated FOXO4 protein showed striking
178 increases in abundance following TS cell differentiation (**Fig. 4E-F**). As previously
179 demonstrated, AKT activity increased following trophoblast cell differentiation (**Kamei et al.,**

180 **2002; Kent et al., 2010, 2011; Fig. 4G**). AKT activation was required for optimal FOXO4
181 phosphorylation (**Fig. 4G**). Intracellular distributions of FOXO4 and phosphorylated FOXO4
182 were affected by inhibition of PI3K in differentiated rat TS cells (**Fig. 4H**). Disruption of
183 PI3K/AKT signaling shifted FOXO4 and phosphorylated FOXO4 to the nucleus (**Fig. 4H**).
184 Inhibition of PI3K in rat TS cells did not significantly impact a measure of apoptosis (cleaved
185 caspase 3) but did show evidence for increased autophagy (**Fig. S2C and D**). Thus, we
186 provide support for a link between PI3K/AKT signaling and FOXO4 in trophoblast cell
187 lineage development.

188

189 **Generation of a *Foxo4* mutant rat model**

190 We examined the role of FOXO4 in regulating placentation in the rat using CRISPR/Cas9
191 genome editing. The *Foxo4* gene consists of four exons and resides on the X chromosome
192 (**Liu et al., 2020**). A mutant rat strain possessing a 3,096 bp deletion within the *Foxo4* gene
193 was generated (**Fig. 5A and B**). The deletion included the 3' part of Exon 2 and the 5' part of
194 Exon 3 and led to a frameshift and a premature stop codon (**Fig. 5A and B**). The deletion
195 effectively disrupted the conserved forkhead DNA binding domain and removed nuclear
196 localization, nuclear export, and transactivation domains of FOXO4 (**Fig. 5C**). The *Foxo4*
197 mutation was successfully transmitted through the germline (**Fig. 5D; Table S4**). A rat colony
198 possessing the *Foxo4* mutation was established and maintained via hemizygous male x wild
199 type female breeding, which produced the predicted Mendelian ratio (**Table S4**). Junctional
200 zone tissues possessing a maternally inherited *Foxo4* mutation (*Foxo4*^{Xm-}) were deficient in
201 FOXO4 protein (**Fig. 5E**). The results are consistent with paternal silencing of X
202 chromosome-linked genes expressed in extraembryonic tissues (**Takagi & Sasaki, 1975;**
203 **West et al., 1978; Hemberger, 2002**). FOXO4 was successfully disrupted in the rat.

204

205 **FOXO4 deficiency results in placentomegaly and a modified junctional zone phenotype**

206 Placentation site phenotypes of mice possessing mutations at the *Foxo4* locus have not
207 been described (**Liu et al., 2020; Hosaka et al., 2004**). Rats possessing a maternally inherited
208 mutant *Foxo4* allele (*Foxo4*^{Xm-}) exhibited placentomegaly and decreased placental efficiency
209 (fetal/placental weight ratio) when examined on gd 18.5 (**Fig. 6A-C**) and gd 20.5 (**Fig**
210 **S3A-C**). In contrast, a paternally inherited mutant *Foxo4* allele did not significantly affect
211 placenta or fetal weights (**Fig S3D and E**). FOXO4 deficiency associated placentomegaly
212 included significantly larger junctional and labyrinth zones (**Fig. 6D-G, Fig S3F-H**) but did
213 not affect the intrauterine invasive trophoblast cell lineage (**Fig S4**). Transcript profiles were
214 determined for wild type (*Foxo4*^{Xm+}) and *Foxo4*^{Xm-} gd 18.5 junctional zone tissues using
215 RNA-seq (**Fig. 6H**). Disruption of FOXO4 resulted in upregulation of 369 transcripts and
216 downregulation of 845 transcripts (**Table S5**). Pathway analysis included signatures for
217 PI3K-AKT signaling, cell cycle, DNA replication, extracellular matrix receptor interaction,
218 and complement and coagulation pathways (**Fig. 6H, Table S6**). Cell cycle and DNA
219 replication signatures may be contributing to the size disparities in wild type (*Foxo4*^{Xm+})
220 versus *Foxo4*^{Xm-} junctional zone compartments. Junctional adhesion molecule-like (**JAML**),
221 lipoprotein(a) like 2 (**LPAL2**), erb-b2 receptor tyrosine kinase 3 (**ERBB3**), and growth factor
222 receptor bound protein 7 (**GRB7**) were each conspicuous in their prominent downregulation
223 (>90% decrease) in FOXO4 deficient junctional zone tissue (**Fig. 6I**). JAML contributes to
224 epithelial barrier function, modulates immune cell trafficking, and angiogenesis (**Kummer &**
225 **Ebnet, 2018**), whereas LPAL2 is a long noncoding RNA contributing to inflammatory and
226 oxidative stress responses (**Han et al., 2018**). JAML and LPAL2 have not previously been
227 linked to trophoblast or placental biology. ERBB3 is a receptor for neuregulin 1 and promotes
228 trophoblast cell survival (**Fock et al., 2015**) and GRB7 is an adaptor protein participating in
229 signal transduction activated through ERBB3 (**Fiddes et al., 1998**). Interestingly, numerous

230 junctional zone transcripts regulated by FOXO4 were reciprocally regulated by AKT1 (88%
231 of transcripts upregulated in *Akt1* null were downregulated in *Foxo4* mutant tissues; 38% of
232 transcripts downregulated in *Akt1* null were upregulated in *Foxo4* mutant tissues; **Fig. 7**). The
233 reciprocal relationship between AKT1 and FOXO4 is evident at structural and molecular
234 levels.

235

236 **FOXO4 contributes to the regulation of the trophoblast cell lineage**

237 We next modeled junctional zone cell biology using rat TS cells. The consequences of
238 FOXO4 disruption in differentiating rat TS cells were examined. FOXO4 expression was
239 inhibited via ectopic expression of short hairpin RNAs specific to *Foxo4* (**Fig. 8A and B**).
240 Although, a morphologic phenotype was not evident, prominent differences in the
241 transcriptomes of TS cells expressing control versus *Foxo4* shRNAs were observed (**Fig. 8C**).
242 Disruption of FOXO4 resulted in upregulation of 260 transcripts and downregulation of 443
243 transcripts (**Table S7**). Pathway analysis included signatures for PI3K-AKT signaling,
244 longevity regulating, calcium signaling, and glutathione metabolism pathways (**Fig. 8C**,
245 **Table S8**). Among the dysregulated transcripts was an upregulation of matrix
246 metalloproteinase 12 (2-fold), a known constituent of endovascular invasive trophoblast cells
247 (**Harris et al., 2010; Chakraborty et al., 2016**) and downregulation of trophoblast specific
248 protein alpha (3-fold), a transcript characteristic of spongiotrophoblast cells within the
249 junctional zone (**Iwatsuki et al., 2000**). FOXO4 is a known regulator of responses to
250 oxidative stress (**Liu et al., 2020**). Several transcripts associated with inflammatory and
251 cellular stress responses, including thioredoxin interacting protein (7-fold), glutathione
252 S-transferase mu 1 (3-fold), arachidonate 5-lipoxygenase activating protein (2-fold),
253 interferon kappa (10-fold), nuclear protein 1 (2.7-fold), and *Lpal2* (2.2-fold), were
254 prominently downregulated (**Sies & Cadenas, 1985; LaFleur et al., 2001; Mashima &**

255 **Okuyama, 2015; Han *et al.*, 2018; Huang *et al.*, 2021; Nirgude & Choudhary, 2021;**
256 **Qayyum *et al.*, 2021; Satapathy & Wilson, 2021).**

257 In vivo and in vitro disruptions of FOXO4 were consequential but did not yield identical
258 transcriptomic effects. These discrepancies may reflect intrinsic differences in the cellular
259 compositions of the gd 18.5 junctional zone versus differentiated rat TS cells, in vivo versus
260 in vitro cell environments, or the null in vivo model versus the hypomorphic in vitro model.

261

262 **Key findings**

263 Collectively, the results indicate that AKT1 drives placental growth, including regulation
264 of deep intrauterine trophoblast cell invasion. These actions are accomplished, at least in part,
265 through modulation of FOXO4, which acts to restrain placental growth and coordinate
266 responses to physiological stressors.

267

268 **DISCUSSION**

269 The rat and human possess a type of hemochorial placentation where specialized
270 trophoblast cells penetrate deep into the uterus and transform the uterine parenchyma,
271 including the vasculature (**Pijnenborg *et al.*, 1981; Pijnenborg & Vercruyse, 2010; Soares
272 *et al.*, 2012**). Central to deep placentation is the source of invasive trophoblast cells, which in
273 the rat is a compartment within the placenta referred as the junctional zone and, in the human,
274 the extravillous trophoblast cell column (**Soares *et al.*, 2012, 2018; Knöfler *et al.*, 2019**). In
275 addition to an intrauterine role, the cellular constituents of these placental compartments
276 produce hormones directed to maternal tissues with actions that ensure in utero survival and
277 promotion of fetal growth (**Soares *et al.*, 1996; John, 2017**). In this report, AKT1 and
278 FOXO4 were identified as regulators of rat junctional zone development. In vivo disruption
279 of AKT1 and FOXO4 led to opposite effects on junctional zone development. AKT1

280 deficiency resulted in growth restriction of the junctional zone, phenotypic alteration of the
281 invasive trophoblast cell lineage, as well as compromised fetal and postnatal growth, and
282 AKT1 was capable of phosphorylating FOXO4 in rat trophoblast cells. Deficiency of FOXO4
283 resulted in an expanded junctional zone. Deficits in AKT1 or FOXO4 also impacted
284 transcriptomic profiles of the junctional zone. The findings indicate that AKT1 and FOXO4
285 are part of a gene regulatory network controlling hemochorial placentation.

286

287 AKT1 signaling influenced placental development. *Akt1* null mutations in the mouse and
288 rat yield similar phenotypes characterized by placental, fetal, and postnatal growth restriction
289 (**Chen et al., 2001; Cho et al., 2001; Yang et al., 2003; Plaks et al., 2011; Kent et al., 2012**).
290 Smaller junctional zones accompanying AKT1 deficiency were associated with a
291 downregulation of transcripts encoding proteins driving cell proliferation. These results imply
292 that size differences of junctional zone compartments in the wild type versus *Akt1* nulls were
293 related to, at least in part, diminished trophoblast cell proliferation in *Akt1* junctional zone
294 tissues. The data also fit well with known actions of AKT signaling promoting cell
295 proliferation in a wide range of cell types (**Manning & Cantley, 2007; Manning & Toker,**
296 **2017; Cole et al., 2019**). AKT1 disruption also altered differentiated junctional zone
297 trophoblast cell phenotypes. As cellular constituents of the junctional zone differentiate, they
298 acquire the capacity to express several members of the expanded prolactin (**PRL**) family of
299 hormones/cytokines (**Soares, 2004; Alam et al., 2006; Soares et al., 2007**). The expression
300 of PRL8A4, a member of the expanded PRL family, was dramatically downregulated in *Akt1*
301 null junctional zones. PRL8A4 is an orphan ligand with little known of its significance to the
302 biology of pregnancy other than as a signature feature of the differentiated junctional zone
303 phenotype (**Iwatsuki et al., 1998; Soares et al., 2007**). AKT signaling has previously been
304 implicated in the regulation of the differentiation of rodent and human trophoblast cells

305 **(Kamei et al., 2003; Kent et al., 2010, 2011; Haslinger et al., 2013)**. Disruption of *Akt1* also
306 interfered with invasive trophoblast cell development. Trophoblast cell infiltration into the
307 uterine-placental interface was diminished in *Akt1* nulls. Involvement of AKT signaling has
308 also been implicated in the development of the human extravillous trophoblast cell lineage
309 **(Pollheimer & Knöfler, 2005; Haslinger et al., 2013; Morey et al., 2021)**. AKT signaling
310 could affect invasive trophoblast cell development through its actions on their origin in the
311 junctional zone and EVT cell column or alternatively, their maturation as they invade into the
312 uterus. Finally, the impact of AKT signaling in invasive trophoblast cell development may be
313 more profound than observed with AKT1 deficiency due to compensatory activities of AKT2
314 and AKT3 **(Kent et al., 2011; Haslinger et al., 2013)**.

315

316 AKT1 regulates cellular function through its actions as a serine/threonine kinase and thus,
317 phosphorylation of its substrates **(Manning & Cantley, 2007; Manning & Toker, 2017;**
318 **Cole et al., 2019)**. The forkhead box (FOX) family of transcription factors are
319 well-established targets of AKT action **(Lam et al., 2013; Schmitt-Ney, 2020; Herman et al.,**
320 **2021)**. Among FOX family members, FOXO4 expression was uniquely elevated in the rat
321 junctional zone. FOXO4 phosphorylation state in trophoblast cells was affected by AKT
322 signaling. AKT-mediated phosphorylation of FOXO4 leads to FOXO4 exit from the nucleus
323 and inactivation **(Schmitt-Ney, 2020; Herman et al., 2021)**, which might suggest that an
324 AKT1 deficiency would result in the stabilization of FOXO4 protein in the junctional zone.
325 Instead, AKT1 deficiency led to depletion of junctional zone total and phosphorylated
326 FOXO4 proteins. Consequently, the observed *Akt1* null placental phenotype was associated
327 with the depletion of both AKT1 and FOXO4 proteins. In addition to regulation by AKT
328 signaling, FOXO4 activity/stability is stimulated by Jun kinase and monoubiquitylation
329 **(Essers et al., 2004; van der Horst et al., 2006; Brenkman et al., 2008; Liu et al., 2020)**,

330 while inhibited by acetylation and polyubiquitylation (**Fukuoka *et al.*, 2003; Huang &**
331 **Tindall, 2011; Liu *et al.*, 2020**). Whether AKT1 indirectly affects FOXO4 protein via
332 impacting these other FOXO4 regulators remains to be determined.

333

334 FOXO4 is a transcription factor implicated in the regulation of the cell cycle, apoptosis,
335 responses to oxidative stress, and a range of disease processes (**Liu *et al.*, 2020**). The original
336 characterization of the *Foxo4* null mouse concluded that FOXO4 did not have a singular role
337 in the pathophysiology of the mouse (**Hosaka *et al.*, 2004**). The absence of a reported
338 phenotype for the *Foxo4* null mouse model was attributed to the compensatory actions of
339 other members of the FOXO family, including FOXO1, FOXO3, and possibly FOXO6
340 (**Hosaka *et al.*, 2004; Liu *et al.*, 2020**). We describe a prominent placental phenotype for the
341 *Foxo4* null rat model. The placental anomalies associated with FOXO4 deficiency were
342 compatible with the production of viable offspring. The absence of a fertility defect in the
343 *Foxo4* null mouse model likely precluded a closer examination of placentation (**Hosaka *et al.*,**
344 **2004**). However, it is also possible that elements of FOXO4 action are species specific.
345 FOXO4 is prominently expressed in the junctional zone and to a lesser extent in invasive
346 trophoblast cells. Disruption of FOXO4 led to an expansion of both junctional and labyrinth
347 zone placental compartments, which probably reflects cell autonomous and non-cell
348 autonomous actions, respectively. A striking reciprocal pattern of AKT1 versus FOXO4 gene
349 regulation within the junctional zone was demonstrated and included differentially regulated
350 transcripts encoding proteins involved in the regulation of cell proliferation and cell death.
351 We surmise that AKT1 promotes junctional zone growth via stimulating the expression of
352 transcripts connected to cell cycle progression and inhibited transcripts connected to cell
353 death, whereas the converse is true for FOXO4. These biological roles are consistent with the
354 known actions of AKT1 and FOXO4 in other cell systems (**Manning & Toker, 2017; Liu *et***

355 *al.*, 2020; Herman *et al.*, 2021). A transcriptional regulatory network involving FOXO4 has
356 also been identified in human extravillous trophoblast cells (Morey *et al.*, 2021). Importantly,
357 FOXO4 also regulates trophoblast cell responses to oxidative stress and is thus, positioned to
358 contribute to placental adaptations to a compromised maternal environment and in disease
359 states affecting placentation.

360

361 **MATERIALS AND METHODS**

362 **Animals**

363 Holtzman Sprague-Dawley rats were maintained in an environmentally controlled facility
364 with lights on from 0600 to 2000 h with food and water available ad libitum. Time-mated
365 pregnancies were established by co-housing adult female rats (8-10 weeks of age) with adult
366 male rats (>10 weeks of age). Detection of sperm or a seminal plug in the vagina was
367 designated gd 0.5. Pseudopregnant females were generated by co-housing adult female rats
368 (8-10 weeks of age) with adult male vasectomized males (>10 weeks of age). The detection
369 of seminal plugs was designated pseudopregnancy day 0.5. Four to five-week-old donor rats
370 were superovulated by intraperitoneal injection of pregnant mare serum gonadotropin (30
371 units, G4877, Sigma-Aldrich, St. Louis, MO), followed by an intraperitoneal injection of
372 human chorionic gonadotropin (30 units, C1063, Sigma-Aldrich) ~46 h later, and
373 immediately mated with adult males. Zygotes were flushed from oviducts the next morning
374 (gd 0.5). The University of Kansas Medical Center (**KUMC**) Animal Care and Use
375 Committee approved all protocols involving the use of rats.

376

377 **Tissue collection and analysis**

378 Rats were euthanized by CO₂ asphyxiation at designated days of gestation. Uterine
379 segments containing placentation sites were frozen in dry ice-cooled heptane and stored at

380 -80°C until processed for histological analyses. Alternatively, placentation sites were
381 dissected into placentas, the adjacent uterine-placental interface tissue (also referred to as the
382 metrial gland), and fetuses as previously described (**Ain et al., 2006**). Placentas were weighed
383 and dissected into junctional zone and labyrinth zone compartments (**Ain et al., 2006**).
384 Placental compartments and uterine-placental interfaces were frozen in liquid nitrogen and
385 stored at -80°C until used for biochemical analyses. Fetuses were weighed, genotyped, and
386 sex determined by polymerase chain reaction (**PCR**) (**Dhakar & Soares, 2017**).

387

388 **Generation of *Akt1* and *Foxo4* mutant rat models**

389 Mutations at *Akt1* and *Foxo4* loci were generated using CRISPR/Cas9 genome editing
390 (**Kaneko, 2017; Iqbal et al., 2021**). Guide RNAs targeting Exon 4 (target sequence:
391 GCCGTTTGAGTCCATCAGCC; nucleotides 356-375) and Exon 7 (target sequence:
392 TTGTCATGGAGTACGCCAAT; nucleotides 712-731) of the *Akt1* gene (NM_033230.3) or
393 targeting Exon 2 (target sequence: CCAGATATACGAATGGATGGTCC; nucleotides
394 517-539) and Exon 3 (target sequence: GTTCATCAAGGTACATAACGAGG; nucleotides
395 631-653) of the *Foxo4* gene (NM_001106943.1) were electroporated into single-cell rat
396 embryos using the NEPA21 electroporator (Nepa Gene Co Ltd, Ichikawa City, Japan).
397 Electroporated embryos were transferred to oviducts of day 0.5 pseudopregnant rats. Initially,
398 offspring were screened for *Akt1* or *Foxo4* mutations from genomic DNA from tail-tip
399 biopsies using the REDExtract-N-AmpTM Tissue PCR kit (XNAT, Millipore Sigma,
400 Burlington, MA). PCR was performed on the purified DNA samples using primers flanking
401 the guide RNA sites, and products resolved by agarose gel electrophoresis and ethidium
402 bromide staining. Genomic DNA containing potential mutations was amplified by PCR, gel
403 purified, and precise boundaries of deletions determined by DNA sequencing (Genewiz Inc.,
404 South Plainfield, NJ). Founders with *Akt1* or *Foxo4* mutations were backcrossed to wild type

405 rats to demonstrate germline transmission. Routine genotyping was performed by PCR on
406 genomic DNA with specific sets of primers (**Table S9**).

407

408 **Western blot analysis**

409 Tissue lysates were prepared with radioimmunoprecipitation assay lysis buffer system
410 (sc-24948A, Santa Cruz Biotechnology, Santa Cruz, CA). Protein concentrations were
411 determined using the *DC*TM Protein Assay Kit (5000112, Bio-Rad Laboratories, Hercules,
412 CA). Proteins (20 µg/lane) were separated by SDS-PAGE. Separated proteins were
413 electrophoretically transferred to polyvinylidene difluoride membranes (10600023, GE
414 Healthcare, Milwaukee, WI) for 1 h at 100 V on ice. Membranes were subsequently blocked
415 with 5% milk or 5% bovine serum albumin for 1 h at room temperature and probed separately
416 with specific primary antibodies to AKT1 (1:1,000 dilution, 75692, Cell Signaling
417 Technology, Danvers, MA), pan-AKT (1:1,000 dilution, 4691, Cell Signaling Technology),
418 phospho-Ser⁴⁷³ AKT (1:2,000 dilution, 4060, Cell Signaling Technology), FOXO4 (1:2,000
419 dilution, 21535-1-AP, Proteintech, Rosemont, IL), phospho-Ser²⁶² FOXO4 (1:3,000 dilution,
420 ab126594, Abcam, Cambridge, MA), cleaved caspase-3 (Asp175, 1:1,000 dilution, 9664, Cell
421 Signaling Technology), serine palmitoyltransferase long chain base subunit 3 (**LC3B**, 1:1,000
422 dilution, 2775, Cell Signaling Technology), and glyceraldehyde 3-phosphate dehydrogenase
423 (**GAPDH**, 1:5,000 dilution, ab8245, Abcam) in Tris-buffered saline with Tween 20 (**TBST**)
424 overnight at 4°C. After primary antibody incubation, the membranes were washed in TBST
425 three times for ten min each at room temperature. After washing, the membranes were
426 incubated with anti-rabbit or anti-mouse immunoglobulin G (**IgG**) conjugated to horseradish
427 peroxidase [**HRP**, 1:5,000 dilution or 1:20,000 dilution (phospho-Ser²⁶² FOXO4), 7074S and
428 7076S, Cell Signaling Technology] in TBST for 1 h at room temperature, washed in TBST
429 three times for ten min each at room temperature, immersed in Immobilon Crescendo

430 Western HRP Substrate (WBLUR0500, Sigma-Aldrich), and luminescence detected using
431 Radiomat LS film (Agfa Healthcare, Mortsel, Belgium) or Chemi Doc MP Imager (Bio-Rad)

432

433 **Transcript analysis**

434 Total RNA was extracted from tissues using TRI Reagent Solution (AM9738,
435 Thermo-Fisher, Waltham, MA) according to the manufacturer's instructions. Total RNA (1
436 μ g) was reverse transcribed using a High-Capacity cDNA Reverse Transcription Kit
437 (4368813, Thermo-Fisher). Complementary DNAs were diluted 1:10 and subjected to reverse
438 transcription-quantitative PCR (**RT-qPCR**) using PowerUp SYBR Green Master Mix
439 (A25742, Thermo-Fisher) and primers provided in **Table S10**. QuantStudio 5 Flex Real-Time
440 PCR System (Applied Biosystems, Foster City, CA) was used for amplification and
441 fluorescence detection. PCR was performed under the following conditions: 95 $^{\circ}$ for 10 min,
442 followed by 40 cycles of 95 $^{\circ}$ for 15 sec and 60 $^{\circ}$ for 1 min. Relative mRNA expression was
443 calculated using the delta-delta Ct method. *Gapdh* was used as a reference transcript.

444

445 **RNA-seq analysis**

446 Transcript profiles were generated from wild type and *Akt1*^{-/-}, and *Foxo4*^{Xm} junctional
447 zone tissues, and rat differentiated TS cells expressing control or *Foxo4* shRNAs.
448 Complementary DNA libraries from total RNA samples were prepared with Illumina TruSeq
449 RNA preparation kits according to the manufacturer's instructions (Illumina, San Diego, CA).
450 RNA integrity was assessed using an Agilent 2100 Bioanalyzer (Santa Clara, CA). Barcoded
451 cDNA libraries were multiplexed onto a TruSeq paired-end flow cell and sequenced (100-bp
452 paired-end reads) with a TruSeq 200-cycle SBS kit (Illumina). Samples were run on an
453 Illumina NovaSeq 6000 sequencer at the KUMC Genome Sequencing Facility. Reads from
454 *.fastq files were mapped to the rat reference genome (Ensembl Rnor_5.0.78) using CLC

455 Genomics Workbench 12.0 (Qiagen, Germantown, MD). Transcript abundance was expressed
456 as transcript per million mapped reads (TPM) and a *P* value of 0.05 was used as a cutoff for
457 significant differential expression. Statistical significance was calculated by empirical
458 analysis of digital gene expression followed by Bonferroni's correction. Pathway analysis
459 was performed using Database for Annotation, Visualization, and Integrated Discovery
460 (**DAVID; Huang *et al.*, 2009**).

461

462 **Immunohistochemistry**

463 Placentation sites were embedded in optimum cutting temperature (**OCT**) compound and
464 sectioned at 10 μ m thickness. Sections were fixed in 4% paraformaldehyde, washed in
465 phosphate buffered saline (pH 7.4) three times for five min each, blocked with 10% normal
466 goat serum (50062Z, Thermo-Fisher), and incubated overnight with primary antibodies: pan
467 cytokeratin (1:300 dilution, F3418, Sigma-Aldrich) to identify trophoblast cells, vimentin
468 (1:300 dilution, sc-6260, Santa Cruz Biotechnology) to distinguish placental compartments,
469 and FOXO4 (1:300 dilution, 21535-1-AP, Proteintech, Rosemont, IL), phospho-Ser²⁶²
470 FOXO4 (1:300 dilution, ab126594, Abcam, Cambridge, MA). After washing with phosphate
471 buffered saline (pH 7.4), sections were incubated with corresponding secondary antibodies:
472 Alexa 568-conjugated goat anti-rabbit IgG (1:500 dilution, A11011, Thermo-Fisher) or Alexa
473 568-conjugated rabbit anti-mouse IgG (1:500 dilution, A9044, Sigma-Aldrich) for 2 h at
474 room temperature. Sections were then stained with DAPI (1/25,000 dilution, D1306,
475 Invitrogen) and mounted using Fluoromount-G mounting media (0100-01, Southern Biotech,
476 Birmingham, AL) and examined microscopically. Fluorescence images were captured on a
477 Nikon 90i upright microscope (Nikon) with a Photometrics CoolSNAP-ES monochrome
478 camera (Roper). The area occupied by cytokeratin-positive cells (invasive trophoblast cells)
479 within the uterine-placental interface was quantified using ImageJ software, as previously

480 described (Nteeba *et al.*, 2020).

481

482 **In situ hybridization**

483 Distributions of transcripts for *Foxo4* and *Prl7b1* were determined on cryosections of rat
484 placentation sites. RNAscope Multiplex Fluorescent Reagent Kit version 2 (Advanced Cell
485 Diagnostics, Newark, CA) was used for in situ hybridization analysis. Probes were prepared
486 to detect *Foxo4* (NM_001106943.1, 1038981-C1, target region: 750-1651) and *Prl7b1*
487 (NM_153738.1, 860181-C2, target region: 28-900). Fluorescence images were captured on a
488 Nikon 80i upright microscope (Nikon) with a Photometrics CoolSNAP-ES monochrome
489 camera (Roper).

490

491 **Rat TS cell culture**

492 Blastocyst-derived rat TS cells (Asanoma *et al.*, 2011) were cultured in Rat TS Cell
493 Medium [RPMI 1640 medium (11875093, Thermo-Fisher), 20% (vol/vol) fetal bovine serum
494 (FBS, Thermo-Fisher), 100 μ M 2-mercaptoethanol (M7522, Sigma-Aldrich), 1 mM sodium
495 pyruvate (11360-070, Thermo-Fisher), 100 μ M penicillin and 50 U/mL streptomycin
496 (15140122, Thermo-Fisher)] supplemented with 70% rat embryonic fibroblast
497 (REF)-conditioned medium prepared as described previously (Asanoma *et al.*, 2011), 25
498 ng/ml fibroblast growth factor 4 (FGF4; 100-31, Peprotech), and 1 μ g/mL heparin (H3149,
499 Sigma-Aldrich). For induction of differentiation, rat TS cells were cultured for 15 days in rat
500 TS medium containing 1% (vol/vol) FBS without FGF4, heparin, and REF-conditioned
501 medium. In some experiments, rat TS cells were exposed to a phosphatidylinositol 3-kinase
502 (PI3K) inhibitor (LY294002, 10 μ M, 9901, Cell Signaling Technology), chloroquine (50 μ M
503 for 24 h, C6628, Sigma-Aldrich), or staurosporine (1 μ M for 3 h, 9953, Cell Signaling
504 Technology) followed by Western blot analysis or immunohistochemistry.

505

506 **Lentivirus construction and production**

507 Lentivirus construction and production were described previously (**Muto *et al.*, 2021;**
508 **Varberg *et al.*, 2021**). Briefly, the lentivirus encoding the shRNA targeting *Foxo4* was
509 constructed using a pLKO.1 vector. shRNA oligo sequences used in the analyses are provided
510 in **Table S11**. Lentiviral packaging vectors were obtained from Addgene and included
511 pMDLg/pRRE (plasmid 12251), pRSV-Rev (plasmid 12253), pMD2.G (plasmid 12259).
512 Lentiviral particles were produced using Attractene (301005, Qiagen) in human embryonic
513 kidney (HEK) 293FT (Thermo-Fisher) cells.

514

515 **Lentiviral transduction**

516 Rat TS cells were incubated with lentiviral particles for 24 h followed by selection with
517 puromycin dihydrochloride (5 µg/mL; A11138-03, Thermo-Fisher) for two days. Cells were
518 then cultured for 1-3 days in Rat TS Cell Medium prior to differentiation.

519

520 **Statistical analysis**

521 Student's *t*-test, Welch's *t*-test, Dunnett's test, or Steel test were performed, where
522 appropriate, to evaluate the significance of the experimental manipulations. Results were
523 deemed statistically significant when $P < 0.05$.

524

525 **ACKNOWLEDGEMENTS**

526 The research was supported by postdoctoral fellowships from the Kansas Idea Network of
527 Biomedical Research Excellence, P20 GM103418 (A.M-I.), Lalor Foundation (K.K., A.M-I.,
528 M.M.), American Heart Association (K.K., M.M.), and an NIH National Research Service
529 Award, HD104495 (R.L.S.) and NIH grants (HD020676, HD079363, HD099638,

530 HD105734), and the Sosland Foundation. We also thank Stacy Oxley and Brandi Miller for
531 administrative assistance.

532

533 **AUTHOR CONTRIBUTIONS**

534 K.K., A.M.-I., and M.J.S. conceived and designed the research; K.K., A.M.-I., K.I.,
535 M.-L.W., R.L.S., M.E.S., M.M. performed experiments; K.K., A.M.-I., K.I., M.R.P., and
536 M.J.S. analyzed the data and interpreted results of experiments; K.K., A.M.-I., and M.J.S.
537 prepared figures and manuscript; All authors read, contributed to editing, and approved the
538 final version of manuscript.

539

540 **CONFLICT OF INTEREST**

541 There is no conflict of interest that could be perceived as prejudicing the impartiality of
542 the research reported.

543

544 **DATA AVAILABILITY**

545 RNA-seq datasets are available at the Gene Expression Omnibus (**GEO**) database,
546 <https://www.ncbi.nlm.nih.gov/geo/> (accession number GSE205831). All data generated and
547 analyzed in this study are included in the published article and supporting files. Resources
548 generated from the research are available from the corresponding author upon reasonable
549 request. AKT1 and FOXO4 mutant rat models are available through the Rat Resource and
550 Research Center (Columbia, MO).

551

552 **REFERENCES**

553 **Ain R, Konno T, Canham LN, Soares MJ** (2006) Phenotypic analysis of the rat placenta.
554 *Methods Mol Med* 121: 295-313

555

556 **Alam SM, Ain R, Konno T, Ho-Chen JK, Soares MJ** (2006) The rat prolactin gene family

557 locus: species-specific gene family expansion. *Mamm Genome* 17: 858-877

558

559 **Aplin JD, Jones CJP** (2021) Cell dynamics in human villous trophoblast. *Hum Reprod*

560 *Update* 27: 904-922

561

562 **Asanoma K, Kubota K, Chakraborty D, Renaud SJ, Wake N, Fukushima K, Soares MJ,**

563 **Rumi MA** (2012) SATB homeobox proteins regulate trophoblast stem cell renewal and

564 differentiation. *J Biol Chem* 287: 2257-2268

565

566 **Asanoma K, Rumi MA, Kent LN, Chakraborty D, Renaud SJ, Wake N, Lee DS, Kubota**

567 **K, Soares MJ** (2011) FGF4-dependent stem cells derived from rat blastocysts differentiate

568 along the trophoblast lineage. *Dev Biol* 351: 110-119

569

570 **Brenkman AB, de Keizer PL, van den Broek NJ, Jochemsen AG, Burgering BM** (2008)

571 Mdm2 induces mono-ubiquitination of FOXO4. *PLoS One* 3: e2819

572

573 **Burton GJ, Fowden AL, Thornburg KL** (2016) Placental origins of chronic disease. *Physiol*

574 *Rev* 96: 1509-1565

575

576 **Burton GJ, Jauniaux E** (2018) Pathophysiology of placental-derived fetal growth restriction.

577 *Am J Obstet Gynecol* 218(Suppl): S745-S761

578

579 **Chakraborty D, Rumi MA, Konno T, Soares MJ** (2011) Natural killer cells direct

580 hemochorial placentation by regulating hypoxia-inducible factor dependent trophoblast
581 lineage decisions. *Proc Natl Acad Sci USA* 108: 16295-16300

582

583 **Chakraborty D, Cui W, Rosario GX, Scott RL, Dhakal P, Renaud SJ, Tachibana M,**
584 **Rumi MA, Mason CW, Krieg AJ, Soares MJ** (2016) HIF-KDM3A-MMP12 regulatory
585 circuit ensures trophoblast plasticity and placental adaptations to hypoxia. *Proc Natl Acad Sci*
586 *USA* 113: E7212-E7221

587

588 **Chen WS, Xu PZ, Gottlob K, Chen ML, Sokol K, Shiyanova T, Roninson I, Weng W,**
589 **Suzuki R, Tobe K, et al.** (2001) Growth retardation and increased apoptosis in mice with
590 homozygous disruption of the *Akt1* gene. *Genes Dev* 15: 2203-2208

591

592 **Cho H, Thorvaldsen JL, Chu Q, Feng F, Birnbaum MJ** (2001) *Akt1/PKB*alpha is required
593 for normal growth but dispensable for maintenance of glucose homeostasis in mice. *J Biol*
594 *Chem* 276: 38349-38352

595

596 **Cole PA, Chu N, Salguero AL, Bae H** (2019) AKTivation mechanisms. *Curr Opin Struct Biol*
597 59: 47-53

598

599 **Dash PR, Whitley GS, Ayling LJ, Johnstone AP, Cartwright JE** (2005) Trophoblast
600 apoptosis is inhibited by hepatocyte growth factor through the Akt and beta-catenin mediated
601 up-regulation of inducible nitric oxide synthase. *Cell Signal* 17: 571-580

602

603 **Dhakal P, Soares MJ** (2017) Single-step PCR-based genetic sex determination of rat tissues
604 and cells. *Biotechniques* 62: 232-233

605

606 **Essers MA, Weijzen S, de Vries-Smits AM, Saarloos I, de Ruiter ND, Bos JL, Burgering**

607 **BM** (2004) FOXO transcription factor activation by oxidative stress mediated by the small

608 GTPase Ral and JNK. *EMBO J* 23: 4802–4812

609

610 **Ferretti C, Bruni L, Dangles-Marie V, Pecking AP, Bellet D** (2007) Molecular circuits

611 shared by placental and cancer cells, and their implications in the proliferative, invasive and

612 migratory capacities of trophoblasts. *Hum Reprod Update* 13: 121-141

613

614 **Fiddes RJ, Campbell DH, Janes PW, Sivertsen SP, Sasaki H, Wallasch C, Daly RJ** (1998)

615 Analysis of Grb7 recruitment by heregulin-activated erbB receptors reveals a novel target

616 selectivity for erbB3. *J Biol Chem* 273: 7717-7724

617

618 **Fisher SJ** (2015) Why is placentation abnormal in preeclampsia? *Am J Obstet Gynecol*

619 213(Suppl): S115-S122

620

621 **Fock V, Plessl K, Draxler P, Otti GR, Fiala C, Knöfler M, Pollheimer J** (2015)

622 Neuregulin-1-mediated ErbB2-ErbB3 signalling protects human trophoblasts against

623 apoptosis to preserve differentiation. *J Cell Sci* 128: 4306-4316

624

625 **Fukuoka M, Daitoku H, Hatta M, Matsuzaki H, Umemura S, Fukamizu A** (2003)

626 Negative regulation of forkhead transcription factor AFX (Foxo4) by CBP-induced acetylation.

627 *Int J Mol Med* 12: 503–508

628

629 **Gardner RL, Beddington RS** (1988) Multi-lineage 'stem' cells in the mammalian embryo. *J*

630 *Cell Sci Suppl* 10: 11-27

631

632 **Han BW, Ye H, Wei PP, He B, Han C, Chen ZH, Chen YQ, Wang WT** (2018) Global

633 identification and characterization of lncRNAs that control inflammation in malignant

634 cholangiocytes. *BMC Genomics* 19: 735

635

636 **Harris LK, Smith SD, Keogh RJ, Jones RL, Baker PN, Knöfler M, Cartwright JE,**

637 **Whitley GS, Aplin JD** (2010) Trophoblast- and vascular smooth muscle cell-derived MMP-12

638 mediates elastolysis during uterine spiral artery remodeling. *Am J Pathol* 177: 2103-2115

639

640 **Haslinger P, Haider S, Sonderegger S, Otten JV, Pollheimer J, Whitley G, Knöfler M**

641 (2013) AKT isoforms 1 and 3 regulate basal and epidermal growth factor-stimulated SGHPL-5

642 trophoblast cell migration in humans. *Biol Reprod* 88: 54

643

644 **Hemberger M** (2002) The role of the X chromosome in mammalian extra embryonic

645 development. *Cytogenet Genome Res* 99: 210-217

646

647 **Herman L, Todeschini AL, Veitia RA** (2021) Forkhead transcription factors in health and

648 disease. *Trends Genet* 37: 460-475

649

650 **Hosaka T, Biggs WH 3rd, Tieu D, Boyer AD, Varki NM, Cavenee WK, Arden KC** (2004)

651 Disruption of forkhead transcription factor (FOXO) family members in mice reveals their

652 functional diversification. *Proc Natl Acad Sci USA* 101: 2975–2980

653

654 **Huang C, Santofimia-Castaño P, Iovanna J** (2021) NUPR1: a critical regulator of the

655 antioxidant system. *Cancers (Basel)* 13: 3670

656

657 **Huang D, Sherman B, Lempicki R** (2009) Systematic and integrative analysis of large gene

658 lists using DAVID bioinformatics resources. *Nat Protoc* 4: 44–57

659

660 **Huang H, Tindall DJ** (2011) Regulation of FOXO protein stability via ubiquitination and

661 proteasome degradation. *Biochim Biophys Acta* 1813: 1961–1964

662

663 **Iqbal K, Pierce SH, Kozai K, Dhakal P, Scott RL, Roby KF, Vyhldal CA, Soares MJ**

664 (2021) Evaluation of placentation and the role of the aryl hydrocarbon receptor pathway in a rat

665 model of dioxin exposure. *Environ Health Perspect* 129: 117001.

666

667 **Iwatsuki K, Oda M, Sun W, Tanaka S, Ogawa T, Shiota K** (1998) Molecular cloning and

668 characterization of a new member of the rat placental prolactin (PRL) family, PRL-like protein

669 H. *Endocrinology* 139: 4976-4983

670

671 **Iwatsuki K, Shinozaki M, Sun W, Yagi S, Tanaka S, Shiota K** (2000) A novel secretory

672 protein produced by rat spongiotrophoblast. *Biol Reprod* 62: 1352-1359

673

674 **John RM** (2017) Imprinted genes and the regulation of placental endocrine function:

675 pregnancy and beyond. *Placenta* 56: 86-90

676

677 **Kamei T, Jones SR, Chapman BM, McGonigle KL, Dai G, Soares MJ** (2002) The

678 phosphatidylinositol 3-kinase/Akt signaling pathway modulates the endocrine differentiation

679 of trophoblast cells. *Mol Endocrinol* 16: 1469-1481

680

681 **Kaneko T** (2017) Genome editing of rat. *Methods Mol Biol* 1630: 101-108.

682

683 **Kent LN, Konno T, Soares MJ** (2010) Phosphatidylinositol 3 kinase modulation of
684 trophoblast cell differentiation. *BMC Dev Biol* 10: 97

685

686 **Kent LN, Ohboshi S, Soares MJ** (2012) Akt1 and insulin-like growth factor 2 (Igf2) regulate
687 placentation and fetal/postnatal development. *Int J Dev Biol* 56: 255-261

688

689 **Kent LN, Rumi MA, Kubota K, Lee DS, Soares MJ** (2011) FOSL1 is integral to
690 establishing the maternal-fetal interface. *Mol Cell Biol* 31: 4801-4813

691

692 **Knipp GT, Audus KL, Soares MJ** (1999) Nutrient transport across the placenta. *Adv Drug*
693 *Deliv Rev* 38: 41-58

694

695 **Knöfler M, Haider S, Saleh L, Pollheimer J, Gamage TKJB, James J** (2019) Human
696 placenta and trophoblast development: key molecular mechanisms and model systems. *Cell*
697 *Mol Life Sci* 76: 3479-3496

698

699 **Kubota K, Kent LN, Rumi MA, Roby KF, Soares MJ** (2015) Dynamic regulation of AP-1
700 transcriptional complexes directs trophoblast differentiation. *Mol Cell Biol* 35: 3163-3177

701

702 **Kummer D, Ebnet K** (2018) Junctional adhesion molecules (JAMs): the JAM-integrin
703 connection. *Cells* 7: 25

704

- 705 **LaFleur DW, Nardelli B, Tsareva T, Mather D, Feng P, Semenuk M, Taylor K, Buergin M,**
706 **Chinchilla D, Roshke V, et al.** (2001) Interferon-kappa, a novel type I interferon expressed in
707 human keratinocytes. *J Biol Chem* 276: 39765-39771
708
- 709 **Lam EW, Brosens JJ, Gomes AR, Koo CY** (2013) Forkhead box proteins: tuning forks for
710 transcriptional harmony. *Nat Rev Cancer* 13: 482-495
711
- 712 **Liu W, Li Y, Luo B** (2020) Current perspective on the regulation of FOXO4 and its role in
713 disease progression. *Cell Mol Life Sci* 77: 651-663
714
- 715 **Maltepe E, Fisher SJ** (2015) Placenta: the forgotten organ. *Annu Rev Cell Dev Biol* 31:
716 523-552
717
- 718 **Manning BD, Cantley LC** (2007) AKT/PKB signaling: navigating downstream. *Cell* 129:
719 1261-1274
720
- 721 **Manning BD, Toker A** (2017) AKT/PKB signaling: navigating the network. *Cell* 169:
722 381-405
723
- 724 **Mashima R, Okuyama T** (2015) The role of lipoxygenases in pathophysiology; new insights
725 and future perspectives. *Redox Biol* 6: 297-310
726
- 727 **Morey R, Farah O, Kallol S, Requena DF, Meads M, Moretto-Zita M, Soncin F, Laurent**
728 **LC, Parast MM** (2021) Transcriptomic drivers of differentiation, maturation, and polyploidy
729 in human extravillous trophoblast. *Front Cell Dev Biol* 9: 702046

730

731 **Muto M, Chakraborty D, Varberg KM, Moreno-Irusta A, Iqbal K, Scott RL, McNally**

732 **RP, Choudhury RH, Aplin JD, Okae H, et al.** (2021) Intersection of regulatory pathways

733 controlling hemostasis and hemochorial placentation. *Proc Natl Acad Sci USA* 118:

734 e2111267118

735

736 **Nirgude S, Choudhary B** (2021) Insights into the role of GPX3, a highly efficient plasma

737 antioxidant, in cancer. *Biochem Pharmacol* 184: 114365

738

739 **Nteeba J, Varberg KM, Scott RL, Simon ME, Iqbal K, Soares MJ** (2020) Poorly controlled

740 diabetes mellitus alters placental structure, efficiency, and plasticity. *BMJ Open Diabetes Res*

741 *Care* 8: e001243

742

743 **Pijnenborg R, Robertson WB, Brosens I, Dixon G** (1981) Trophoblast invasion and the

744 establishment of haemochorial placentation in man and laboratory animals. *Placenta* 2:

745 71-91

746

747 **Pijnenborg R, Vercruysse L** (2010) Animal models of deep trophoblast invasion. In

748 *Placental Bed Disorders*, Pijnenborg R, Brosens I, Romero R (eds) pp 127-139. Cambridge:

749 Cambridge University Press

750

751 **Plaks V, Berkovitz E, Vandoorne K, Berkutzki T, Damari GM, Haffner R, Dekel N,**

752 **Hemmings BA, Neeman M, Harmelin A** (2011) Survival and size are differentially regulated

753 by placental and fetal PKBalpha/AKT1 in mice. *Biol Reprod* 84: 537-545

754

755 **Pollheimer J, Knöfler M** (2005) Signalling pathways regulating the invasive differentiation of
756 human trophoblasts: a review. *Placenta* 26(Suppl A): S21-S30

757

758 **Qayyum N, Haseeb M, Kim MS, Choi S** (2021) Role of thioredoxin-interacting protein in
759 diseases and its therapeutic outlook. *Int J Mol Sci* 22: 2754

760

761 **Qiu Q, Yang M, Tsang BK, Gruslin A** (2004) Both mitogen-activated protein kinase and
762 phosphatidylinositol 3-kinase signalling are required in epidermal growth factor-induced
763 human trophoblast migration. *Mol Hum Reprod* 10: 677-684

764

765 **Roberts RM, Green JA, Schulz LC** (2016) The evolution of the placenta. *Reproduction* 152:
766 R179-R189

767

768 **Satapathy S, Wilson MR** (2021) The dual roles of clusterin in extracellular and intracellular
769 proteostasis. *Trends Biochem Sci* 46: 652-660

770

771 **Schmitt-Ney M** (2020). The FOXO's advantages of being a family: considerations on function
772 and evolution. *Cells* 9: 787

773

774 **Sharma N, Kubaczka C, Kaiser S, Nettersheim D, Mughal SS, Riesenberger S, Hölzel M,**

775 **Winterhager E, Schorle H** (2016) Tpbpa-Cre-mediated deletion of TFAP2C leads to
776 deregulation of Cdkn1a, Akt1 and the ERK pathway, causing placental growth arrest.

777 *Development* 143: 787-798

778

779 **Shukla V, Soares MJ** (2022) Modeling trophoblast cell-guided uterine spiral artery

780 transformation in the rat. *Int J Mol Sci* 23: 2947

781

782 **Sies H, Cadenas E** (1985) Oxidative stress: damage to intact cells and organs. *Philos Trans R*

783 *Soc Lond B Biol Sci* 311: 617-631

784

785 **Soares MJ** (2004) The prolactin and growth hormone families: pregnancy-specific

786 hormones/cytokines at the maternal-fetal interface. *Reprod Biol Endocrinol* 2: 51

787

788 **Soares MJ, Chakraborty D, Rumi MAK, Konno T, Renaud SJ** (2012) Rat placentation:

789 an experimental model for investigating the hemochorial maternal-fetal interface. *Placenta*

790 33: 233-243

791

792 **Soares MJ, Chapman BM, Rasmussen CA, Dai G, Kamei T, Orwig KE** (1996)

793 Differentiation of trophoblast endocrine cells. *Placenta* 17: 277-289

794

795 **Soares MJ, Konno T, Alam SM** (2007) The prolactin family: effectors of

796 pregnancy-dependent adaptations. *Trends Endocrinol Metab* 18: 114-121

797

798 **Soares MJ, Varberg KM, Iqbal K** (2018) Hemochorial placentation: development, function,

799 and adaptations. *Biol Reprod* 99: 196-211

800

801 **Takagi N, Sasaki M** (1975) Preferential inactivation of the paternally derived X chromosome

802 in the extraembryonic membranes of the mouse. *Nature* 256: 640-642

803

804 **van der Horst A, de Vries-Smiths AM, Brenkman AB, van Triest MH, van den Broek N,**

805 **Colland F, Maurice MM, Burgering BM** (2006) FOXO4 transcriptional activity is regulated
806 by monoubiquitination and USP7/HAUSP. *Nat Cell Biol* 8: 1064–1073

807

808 **Varberg KM, Iqbal K, Muto M, Simon ME, Scott RL, Kozai K, Choudhury RH, Aplin**
809 **JD, Biswell R, Gibson M, et al.,** (2021) ASCL2 reciprocally controls key trophoblast lineage
810 decisions during hemochorial placenta development. *Proc Natl Acad Sci USA* 118:
811 e2016517118

812

813 **West JD, Papaioannou VE, Frels WI, Chapman VM** (1978) Preferential expression of the
814 maternally derived X chromosome in extraembryonic tissues of the mouse. *Basic Life Sci* 12:
815 361-377

816

817 **Wooding P & Burton G** (2008) *Comparative Placentation*. Springer-Verlag, Heidelberg,
818 Germany

819

820 **Yang ZZ, Tschopp O, Hemmings-Mieszczak M, Feng J, Brodbeck D, Perentes E,**
821 **Hemmings BA** (2003) Protein kinase B alpha/Akt1 regulates placental development and fetal
822 growth. *J Biol Chem* 278: 32124-32131

823

824

825 **FIGURE LEGENDS**

826 **Figure 1. In vivo genome editing of the rat *Akt1* locus. A)** Schematic representation of the
827 rat *Akt1* gene (*Akt1*^{+/+}) and guide RNA target sites within Exons 4 and 7 (NM_033230.3). Red
828 bars beneath Exons 4 and 7 correspond to the 5' and 3' guide RNAs used in the genome
829 editing. **B)** The mutant *Akt1* allele (*Akt1*^{-/-}) possesses a 1,332 bp deletion. Parts of Exons 4

830 and 7 and all of Exons 5 and 6 are deleted, leading to a frameshift and premature Stop codon
831 in Exon 7. **C)** Amino acid sequences for AKT1^{+/+} and AKT1^{-/-}. The red sequence corresponds
832 to the frameshift in Exon 7. The blue, red, and green highlighted amino acid sequence regions
833 correspond to the pleckstrin homology (**PH**), kinase, and regulatory domains, respectively. **D)**
834 Offspring were backcrossed to wild type rats, and heterozygous mutant rats were intercrossed
835 to generate homozygous mutants. Wild type (+/+), heterozygous (+/-), and homozygous
836 mutant (-/-) genotypes were detected by PCR. **E)** Western blot analysis of AKT1, pan-AKT,
837 phospho (p)-AKT (Ser⁴⁷³) protein in *Akt1*^{+/+} and *Akt1*^{-/-} placentas at gd 18.5. GAPDH was
838 used as a loading control.

839

840 **Figure 2. *Akt1*^{-/-} placentas and fetuses are growth restricted, and *Akt1*^{-/-} rats exhibit**
841 **postnatal growth restriction.** Placentas (**A**) and fetuses (**B**) were dissected from *Akt1*^{+/-}
842 intercrosses at gd 18.5 and weighed; **C**, fetus/placenta ratio. Placentas were then separated
843 into junctional zone (**JZ**; **D**) and labyrinth zone (**LZ**;**E**) compartments, and weighed; **F**, JZ/JZ
844 ratio. Graphs represent means ± SEM. *Akt1*^{+/+}, n = 22 from 6 dams; *Akt1*^{-/-}, n = 17 from 6
845 dams. Asterisks denote statistical differences (***P* < 0.01; ****P* < 0.001) as determined by
846 Student's or Welch's *t*-test. Body weights of *Akt1*^{+/+} and *Akt1*^{-/-} pups were measured from two
847 to eight weeks after birth: males (**G**) and females (**H**). Graphs represent means ± SEM. n =
848 13-23/group. Asterisks denote statistical differences (**P* < 0.05; ****P* < 0.001) as determined
849 by Student's or Welch's *t*-test. **I)** Vimentin immunostaining of gd 18.5 *Akt1*^{+/+} and *Akt1*^{-/-}
850 placentation sites. The junctional zone (**JZ**) is negative for vimentin immunostaining,
851 whereas the uterine-placental interface (**UPI**) and labyrinth zone (**LZ**) stain positive for
852 vimentin. Scale bars=1000 μm

853

854 **Figure 3. AKT1 regulates junctional zone and invasive trophoblast cell phenotypes.**

855 **A)** Heat maps depicting differentially expressed genes between *Akt1*^{+/+} and *Akt1*^{-/-} junctional
856 zones. The heatmap color keys represent z-scores of TPM values. **B)** RT-qPCR validation of
857 RNA-seq results (n=6/group). **C)** Schematic representation of a late gestation placentation
858 site. The uterine-placental interface (UPI), site for intrauterine trophoblast invasion, is
859 highlighted in the boxed area. **D)** AKT1 deficiency affected intrauterine trophoblast cell
860 invasion. Trophoblast cells were immunostained for pan-cytokeratin (KRT). Representative
861 images are shown. The extent of intrauterine trophoblast invasion is demarcated using a green
862 dashed line. Scale bars =500 μ m. The white dotted line represents the outer border of the
863 uterus, and the yellow dashed line represents the uterine border with the placenta. **E)** The area
864 of intrauterine trophoblast invasion is graphically depicted (n = 6/group). Graphs represent
865 means \pm SEM. An asterisk denotes statistical difference (**P* < 0.05) as determined by
866 Student's *t*-test. **F)** RT-qPCR measurements of *Krt7* and *Krt8* transcripts, signature markers
867 for invasive trophoblast cells, within dissected uterine-placental interface tissue specimens at
868 gd 18.5 (*Akt1*^{+/+}, n = 21; *Akt1*^{-/-}, n = 16). Graphs represent means \pm SEM. Asterisks denote
869 statistical difference (**P* < 0.05; ***P* < 0.01; ****P* < 0.001) as determined by Student's or
870 Welch's *t*-test.

871

872 **Figure 4. FOXO4 is a target of PI3K/AKT signaling.** **A)** Expressions of transcripts for
873 several FOX transcription factors in the junctional zone. **B)** *In situ* localization of transcripts
874 for *Foxo4* with *Prl7b1* (invasive trophoblast-specific transcript) in the placentation site at gd
875 18.5 of rat pregnancy. Scale bars = 1000 μ m. **C)** RT-qPCR measurements of *Foxo4*
876 transcripts in the uterine-placental interface, junctional and labyrinth zones during the second
877 half of gestation (n = 6-9/group). Graphs represent means \pm SEM. Asterisks denote statistical
878 difference (***P* < 0.01) as determined by Steel test. UPI: uterine-placental interface; JZ:
879 junctional zone; and LZ: labyrinth zone. **D)** Western blot analysis of phospho (p)-FOXO4

880 (Ser²⁶²) and FOXO4 proteins in *Akt1*^{+/+} and *Akt1*^{-/-} placentas at gd 18.5. GAPDH was used as
881 a loading control. **E)** RT-qPCR measurements of *Foxo4* transcripts in the stem state and
882 following induction of differentiation (n = 4-6/group). Graphs represent means ± SEM.
883 Asterisks denote statistical difference (vs Stem, **P* < 0.05) as determined by Dunnett's test.
884 Western blot analysis of phospho (p)-FOXO4 (Ser²⁶²), FOXO4, p-AKT (Ser⁴⁷³), and
885 pan-AKT proteins in the stem and differentiating (day 15 of differentiation, D15) states (**F**),
886 and in the differentiating state (D15) following treated with vehicle (0.1% DMSO) or a
887 phosphatidylinositol 3-kinase (**PI3K**) inhibitor (LY294002, 10 μM) for 1 h (**G**). GAPDH was
888 used as a loading control. **H)** Rat TS following 15 days in differentiating conditions were
889 treated with vehicle (0.1% DMSO, Control) or a phosphatidylinositol 3-kinase (**PI3K**)
890 inhibitor (LY294002, 10 μM) for 24 h and then immunostained for phospho (p)-FOXO4
891 (Ser²⁶²), FOXO4. Representative images are shown. Scale bars =50 μm.

892

893 **Figure 5. In vivo genome editing of the rat *Foxo4* locus.** **A)** Schematic representation of
894 the rat *Foxo4* gene (*Foxo4*^{Xm+}) and guide RNA target sites within Exons 2 and 3
895 (NM_001106943.1). Red bars beneath Exons 2 and 3 correspond to the 5' and 3' guide RNAs
896 used in the genome editing. **B)** The mutant *Foxo4* allele (*Foxo4*^{Xm-}) possesses a 3,096 bp
897 deletion. Parts of Exons 2 and 3 are deleted, leading to a frameshift and premature Stop
898 codon in Exon 3. **C)** Amino acid sequences for FOXO4^{Xm+} and FOXO4^{Xm-}. The red sequence
899 corresponds to the frameshift in Exon 3. The green, red, dark blue, and light blue highlighted
900 amino acid sequence regions correspond to the forkhead winged-helix DNA-binding domain
901 (**FHD**), nuclear localization sequence (**NLS**), nuclear export sequence (**NES**), and
902 transactivation domain (**TAD**), respectively. **D)** Heterozygous mutant female rats were
903 crossed to wild type male rats to generate hemizygous null male rats. Wild type (+/+),
904 heterozygous (+/-), and hemizygous null (-/γ) genotypes were detected by PCR. **E)** Western

905 blot analysis of FOXO4 protein in the junctional zone of *Foxo4*^{Xm+} (X^{m+}Y and X^{m+}X^{P+}) and
906 *Foxo4*^{Xm-} (X^{m-}Y and X^{m-}X^{P+}) placentas at gd 18.5. GAPDH was used as a loading control.

907

908 **Figure 6. *Foxo4* hemizygous null and *Foxo4* maternally inherited heterozygous**
909 **conceptuses exhibit placental overgrowth, and FOXO4 deficiency alters the**
910 **transcriptomes of the junctional zone.** Placentas (A) and fetuses (B) were dissected from
911 *Foxo4* heterozygous females mated with wild type males at gd 18.5 and weighed; C)
912 fetus/placenta ratio. Placentas were then separated into junctional zone (JZ, D) and labyrinth
913 zone (LZ, E) compartments, and weighed; F, JZ/LZ weight ratio. Graphs represent means ±
914 SEM. X^{m+}Y, n = 25; X^{m-}Y, n = 31; X^{m+}X^{P+}, n = 14; X^{m-}X^{P+}, n = 22 from 8 dams. Asterisks
915 denote statistical differences (***) $P < 0.001$ as determined by Student's or Welch's *t*-test. G)
916 Vimentin immunostaining of gd 18.5 *Foxo4*^{Xm+} and *Foxo4*^{Xm-} placentation sites. The
917 junctional zone (JZ) is negative for vimentin immunostaining, whereas the uterine-placental
918 interface (UPI) and labyrinth zone (LZ) stain positive for vimentin. Scale bars=1000 μm. H)
919 Heat maps depicting differentially expressed genes in *Foxo4*^{Xm+} versus *Foxo4*^{Xm-} junctional
920 zones. The heatmap color keys represent z-scores of TPM values. I) RT-qPCR validation of
921 RNA-seq results (n=6/group). Graphs represent means ± SEM. Asterisks denote statistical
922 difference (** $P < 0.01$; *** $P < 0.001$) as determined by Student's or Welch's *t*-test.

923

924 **Figure 7. Reciprocal relationship between AKT1 and FOXO4 in the junctional zone.**

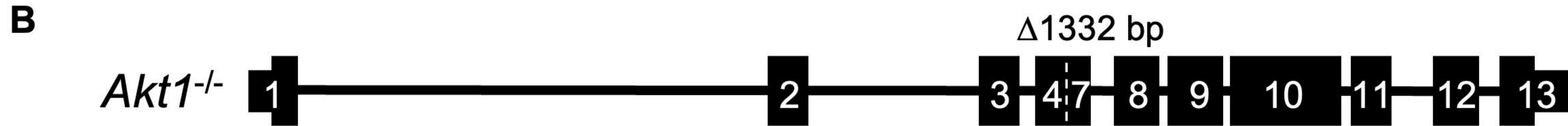
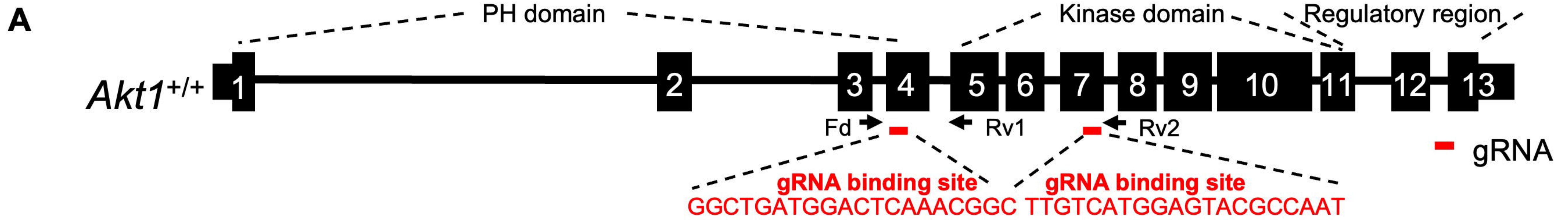
925 Venn diagram and heatmaps representing overlap of differentially expressed genes inversely
926 regulated by AKT1 and FOXO4. The heatmap color keys represent z-scores of TPM values.

927

928 **Figure 8. FOXO4 alters the rat TS cell.** FOXO4 knockdown efficiency was validated by

929 RT-qPCR (A, n = 4/group) or western blot (B) analyses in rat TS cells at day 15 of

930 differentiation following transduction with lentivirus containing a control shRNA or one of
931 two independent *Foxo4*-specific shRNAs. Graphs represent means \pm SEM. Asterisks denote
932 statistical difference (vs Control shRNA, $*P < 0.05$) as determined by Student's or Welch's
933 *t*-test. **C)** Heatmap depicting differentially expressed genes between control and *Foxo4*
934 shRNA-treated rat TS cells. **D)** RT-qPCR validation of RNA-seq results (Control shRNA, n =
935 4; *Foxo4* shRNA 1, n = 4; *Foxo4* shRNA 2, n = 4). Graphs represent means \pm SEM. Asterisks
936 denote statistical difference (compared to Control shRNA, $*P < 0.05$; $**P < 0.01$; $***P <$
937 0.001) as determined by Student's or Welch's *t*-test.
938



C bioRxiv preprint doi: <https://doi.org/10.1101/2022.06.15.496110>; this version posted November 22, 2022. The copyright holder for this preprint (which was not certified by peer review) is the author/funder, who has granted bioRxiv a license to display the preprint in perpetuity. It is made available under aCC-BY-NC-ND 4.0 International license.

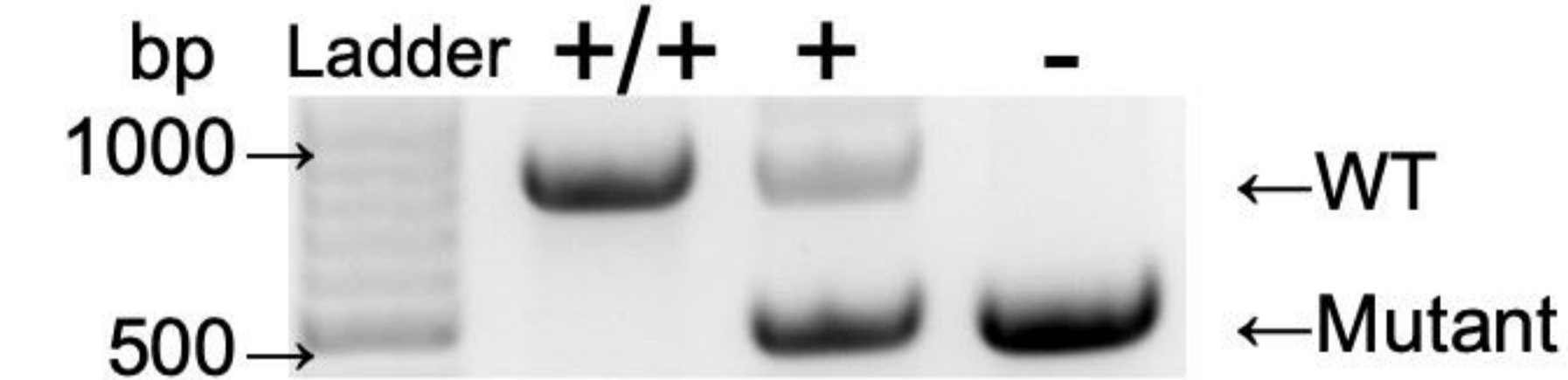
AKT1^{+/+}

MNDVAIVKEGWLHKRGEYIKTWRPRYFLLKNDGTFIGYKERP
 QDVEQRESPLNNFSVAQCQLMKTERPRPNTFIIRCLQWTTVIE
 RTFHVETPEEREEWTTAIQTVADGLKRQEEETMDFRSGSPSD
 NSGAEEMEVALAKPKHRVTMNEFEYLLKLLGKGTFGKVLVKEK
 ATGRYYAMKILKKEVIVAKDEVAHTLTENRVLQNSRHPFLTAL
 KYSFQTHDRLCFVMEYANGGELFFHLSRERVFSEDRARFYGA
 EIVSALDYLHSEKNVVYRDLKLENLMLDKDGHKITDFGLCKEG
 IKDGATMKTFCGTPEYLAPEVLEDNDYGRAVDWWGLGVVMY
 EMMCGRLPFYNQDHEKLFELILMEEIRFPRTLGPPEAKSLLSGL
 LKKDPTQRLGGGSEDAKEIMQHRFFANIVWQDVYEKKLSPPF
 KPQVTSETDTRYFDEEFTAQMITITPPDQDDSMECVDSERRP
 HFPQFSYSASGTA

AKT1^{-/-}

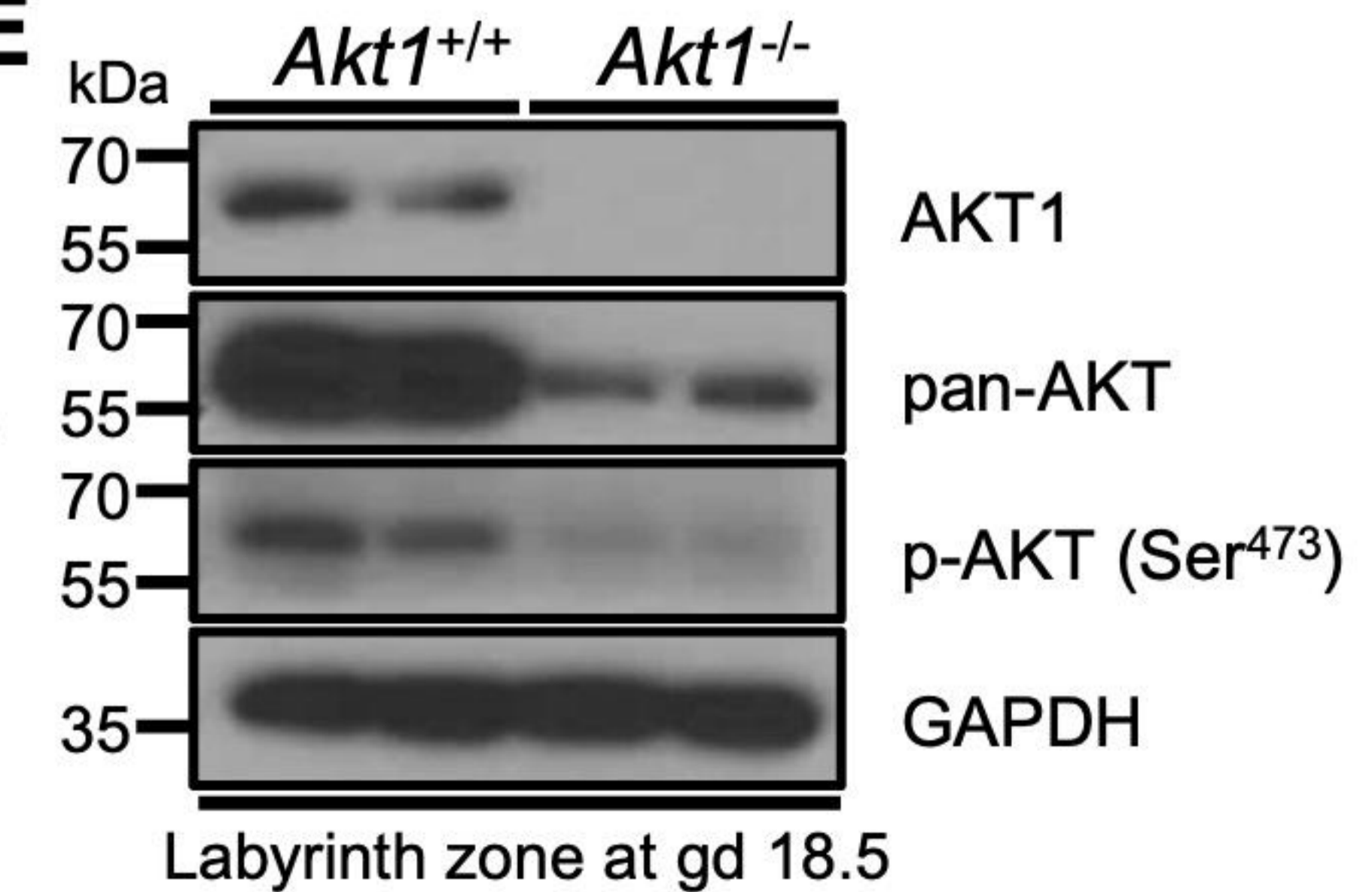
MNDVAIVKEGWLHKRGEYIKTWRPRYFLLKNDGTFIGYKERP
 QDVEQRESPLNNFSVAQCQLMKTERPRPNTFIIRCLQWTTVIE
 RTFHVETPEEREEWTTAIQTVADGLKQWGRALLPPVS Stop

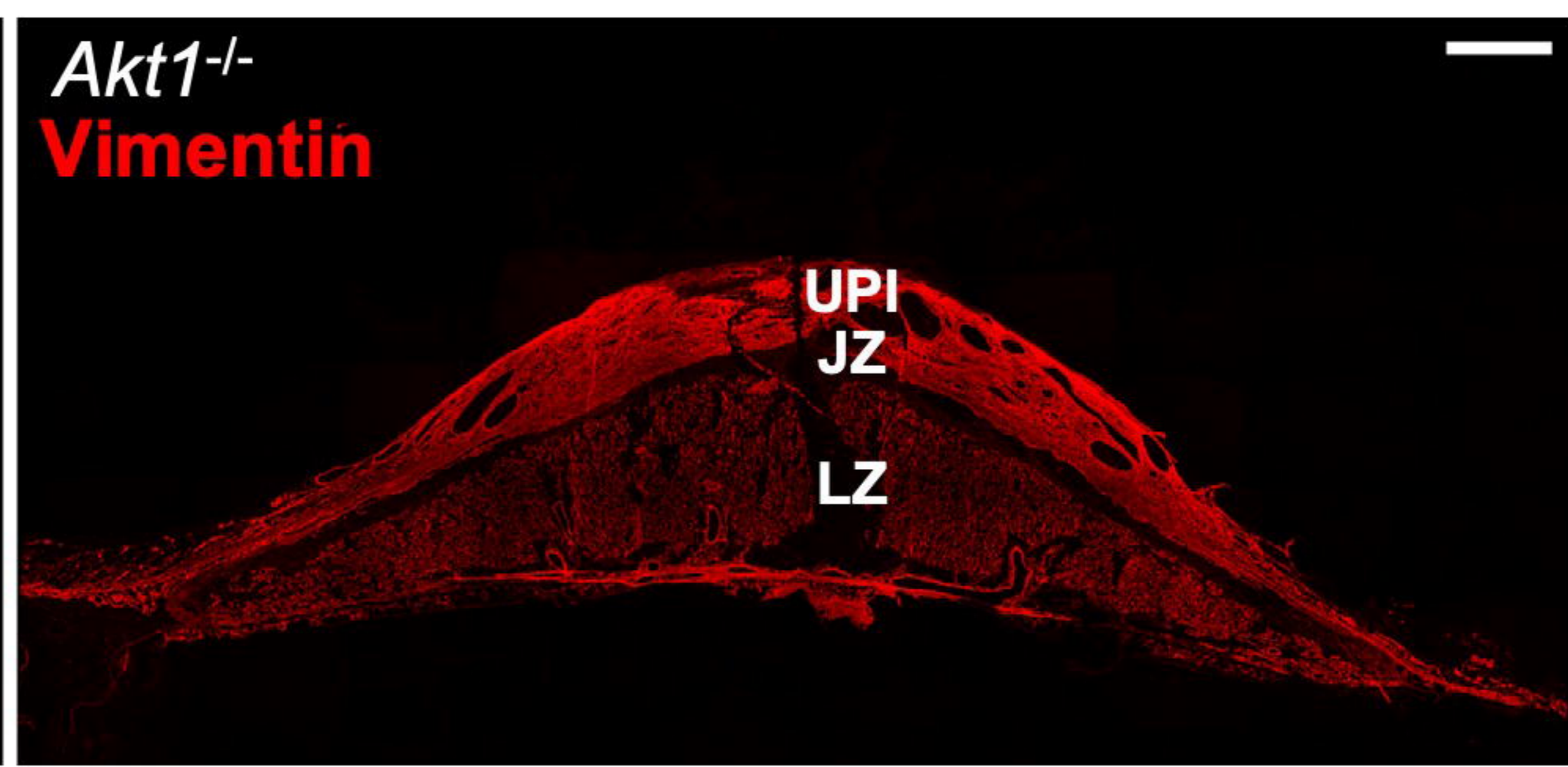
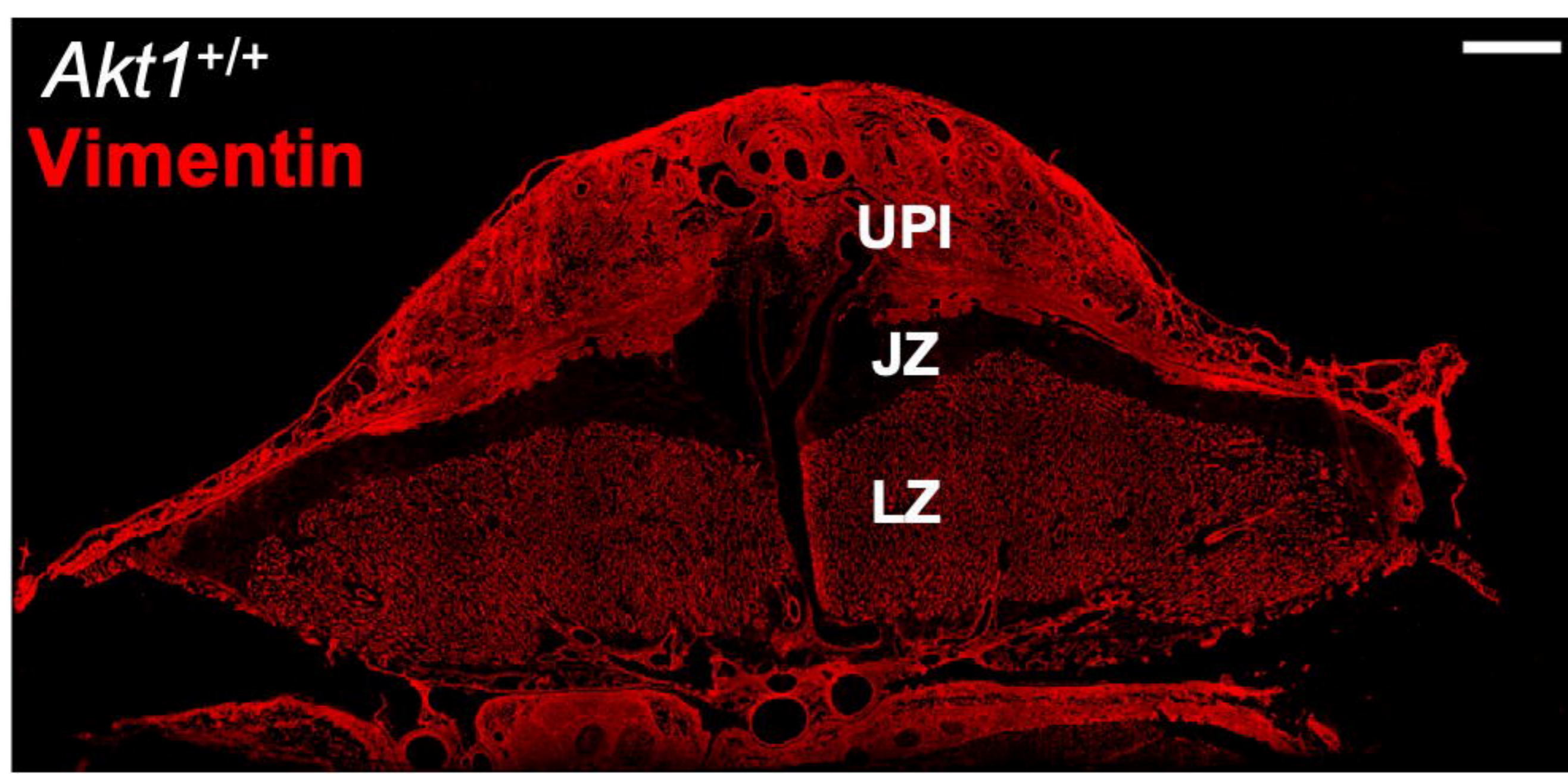
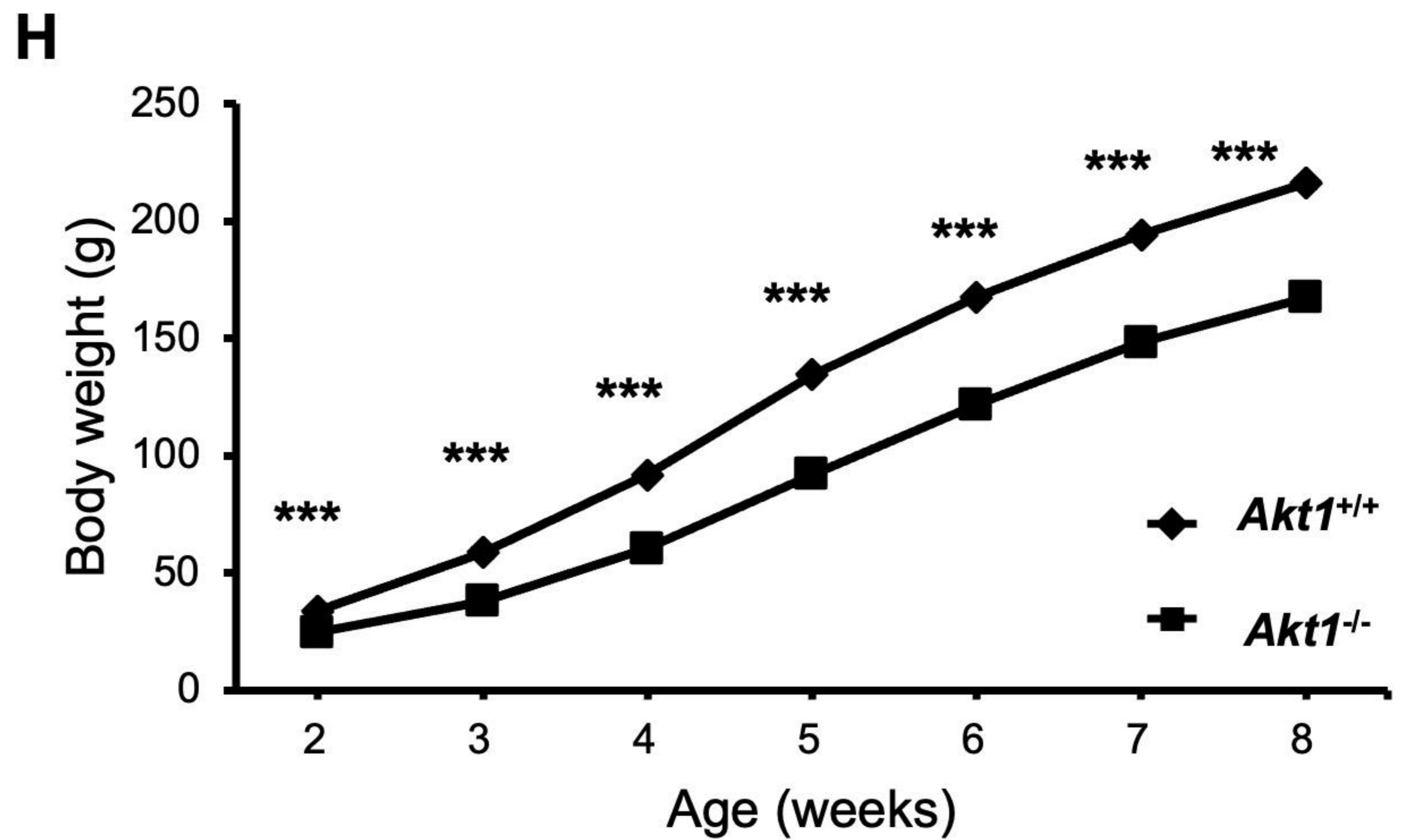
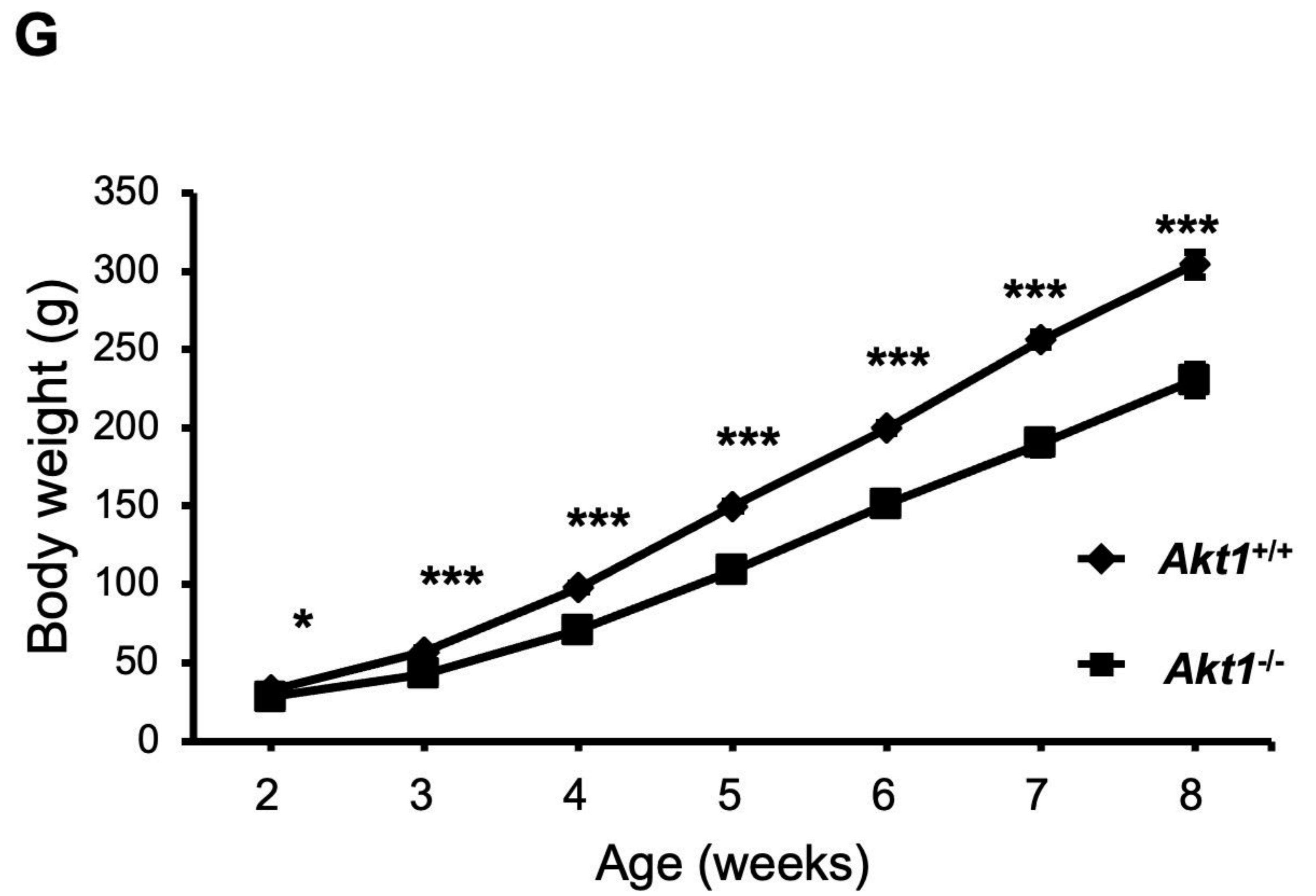
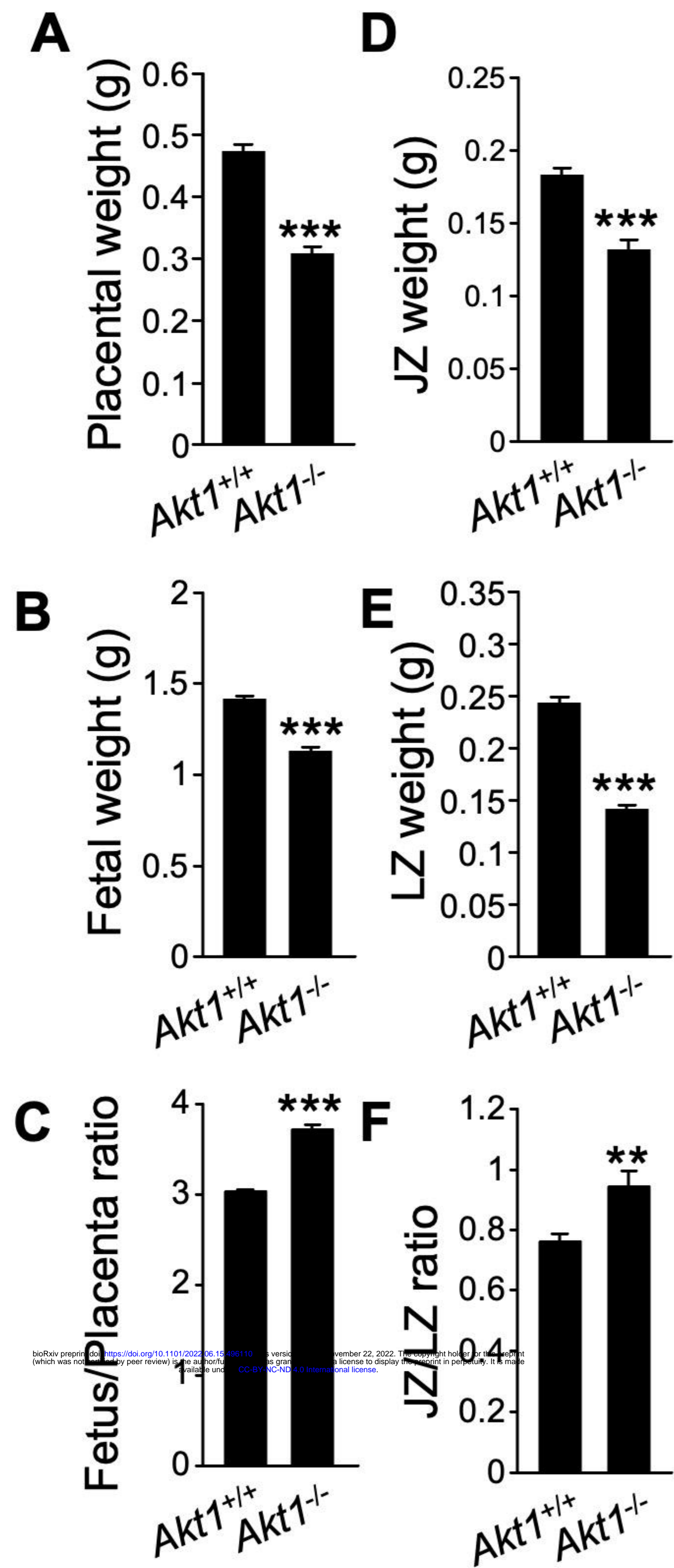
D

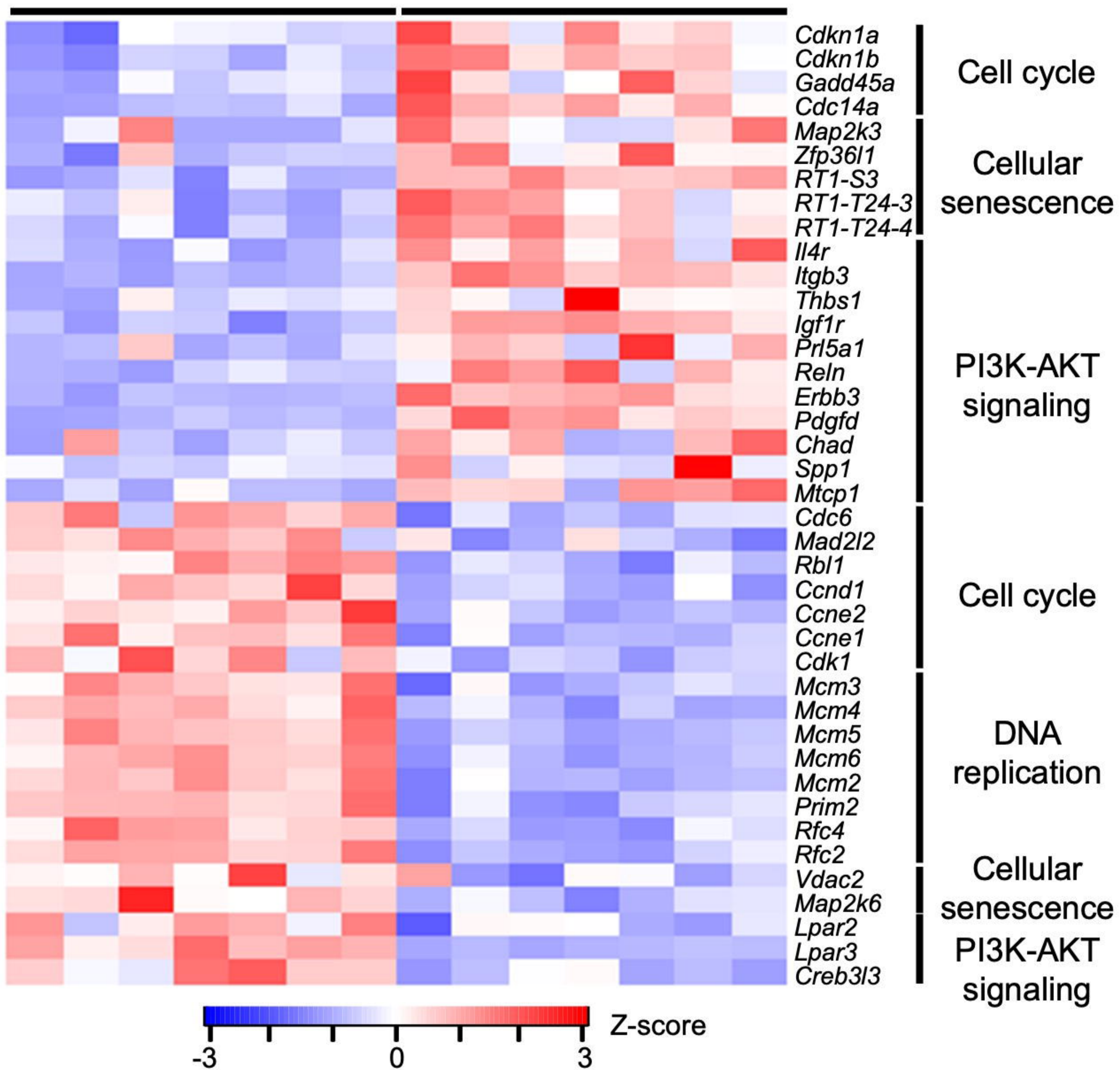
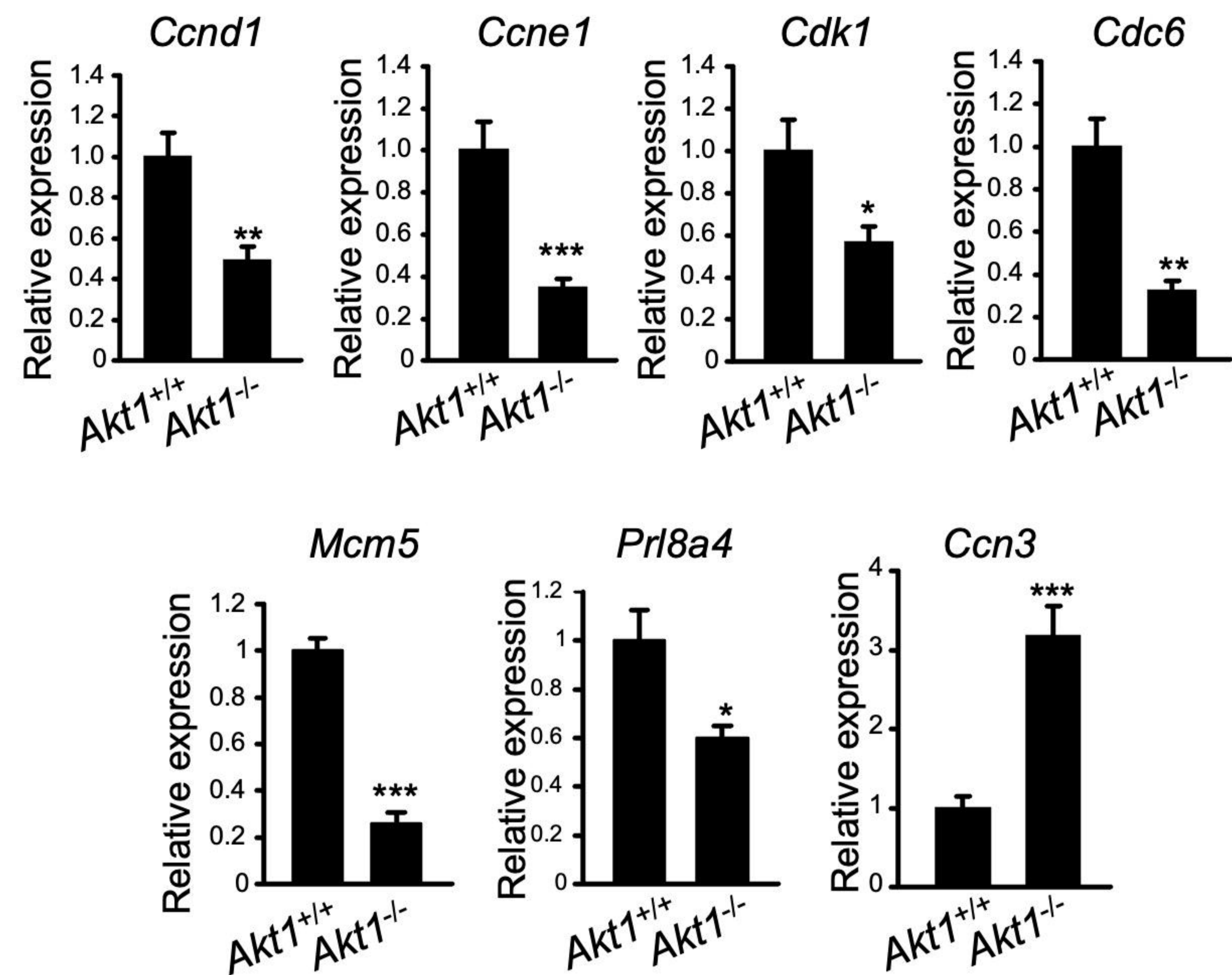
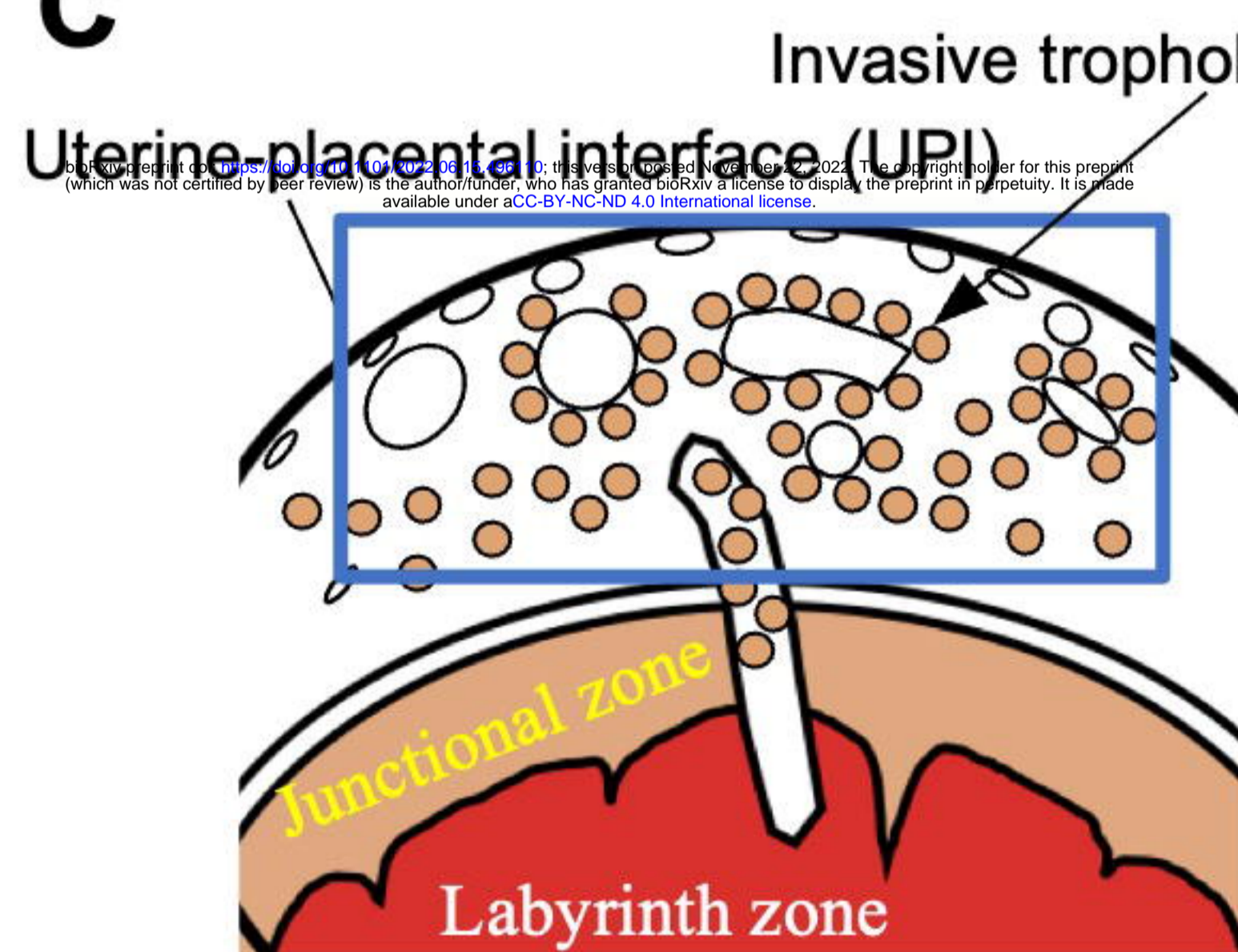
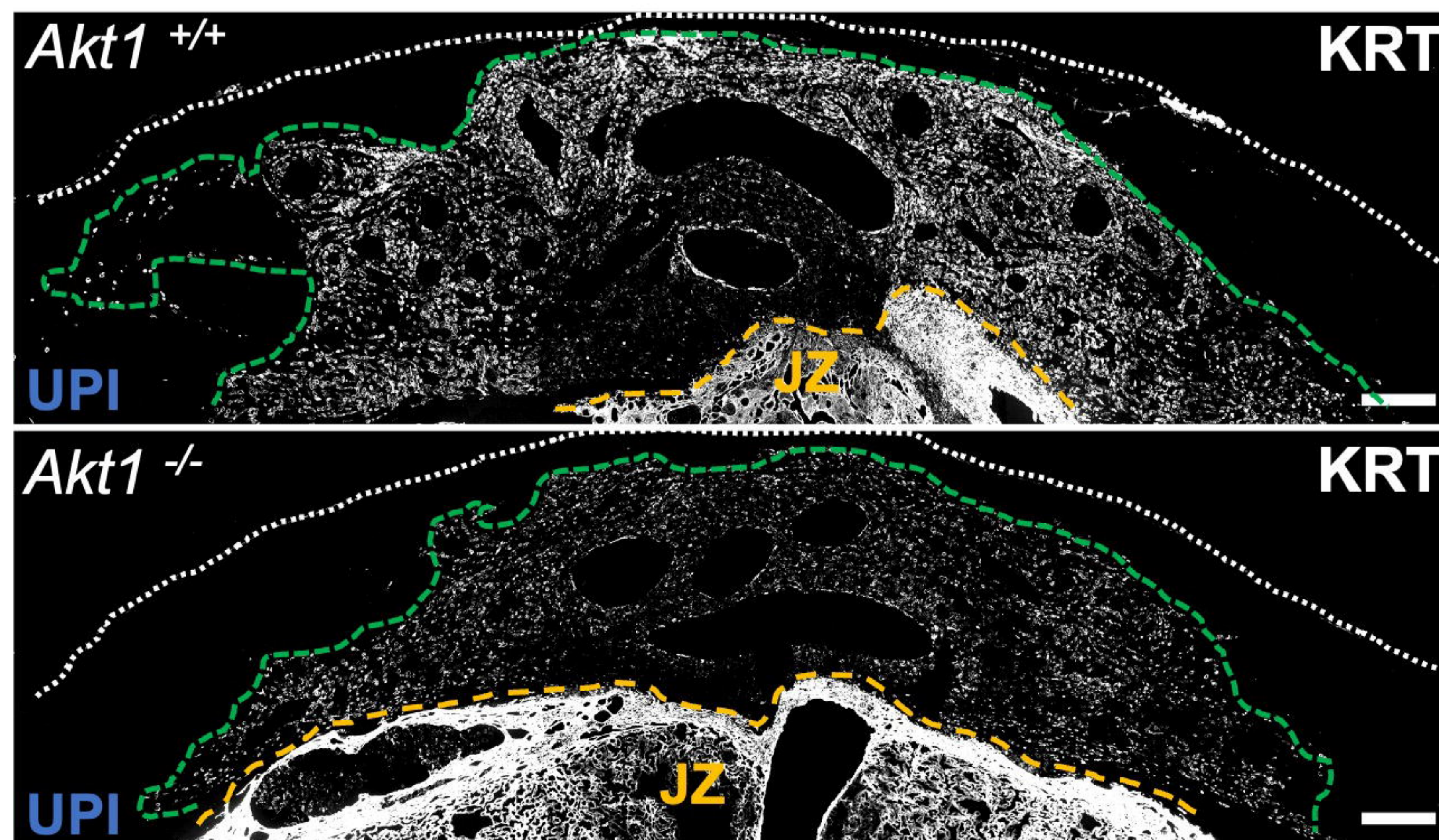
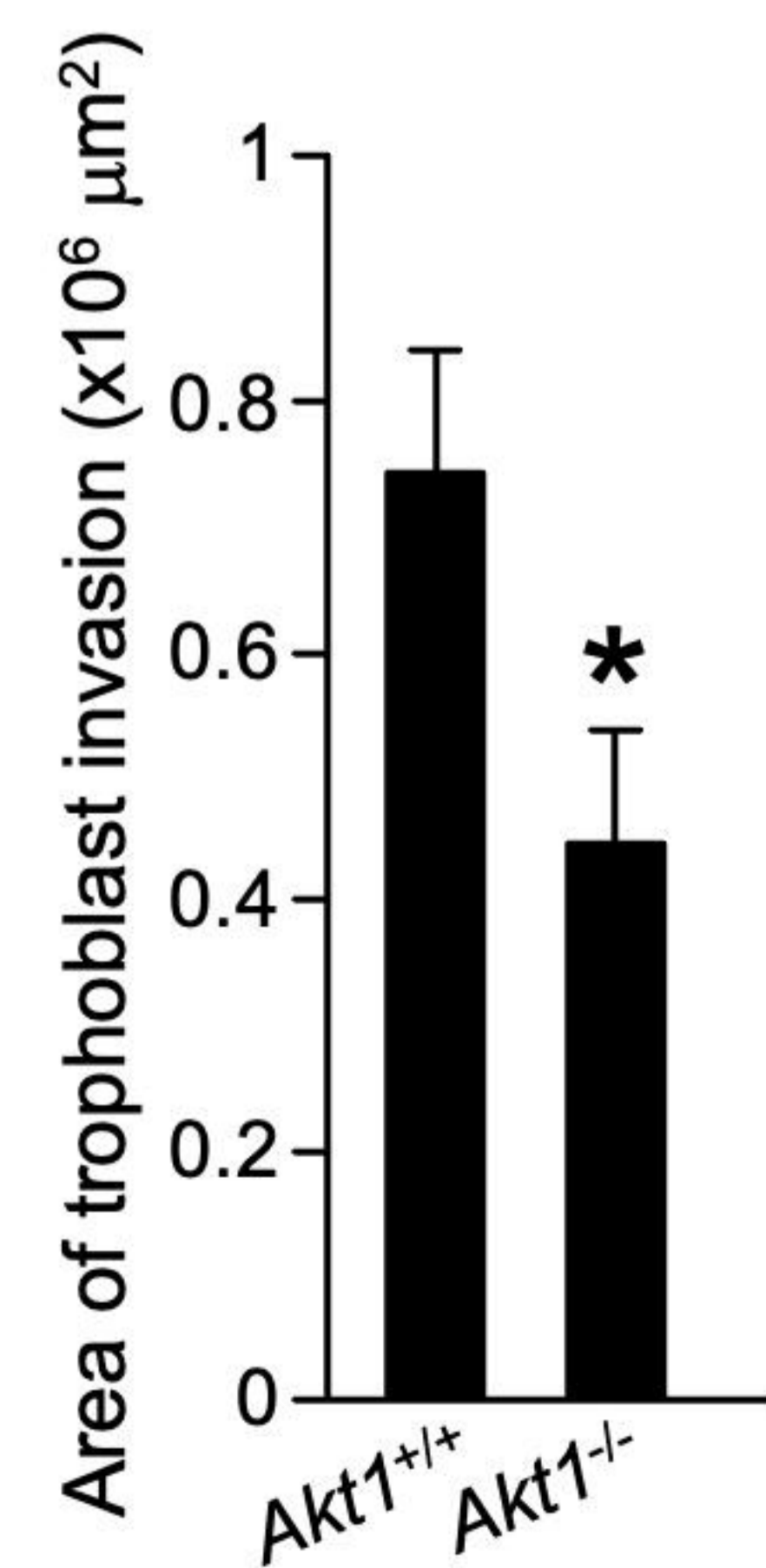
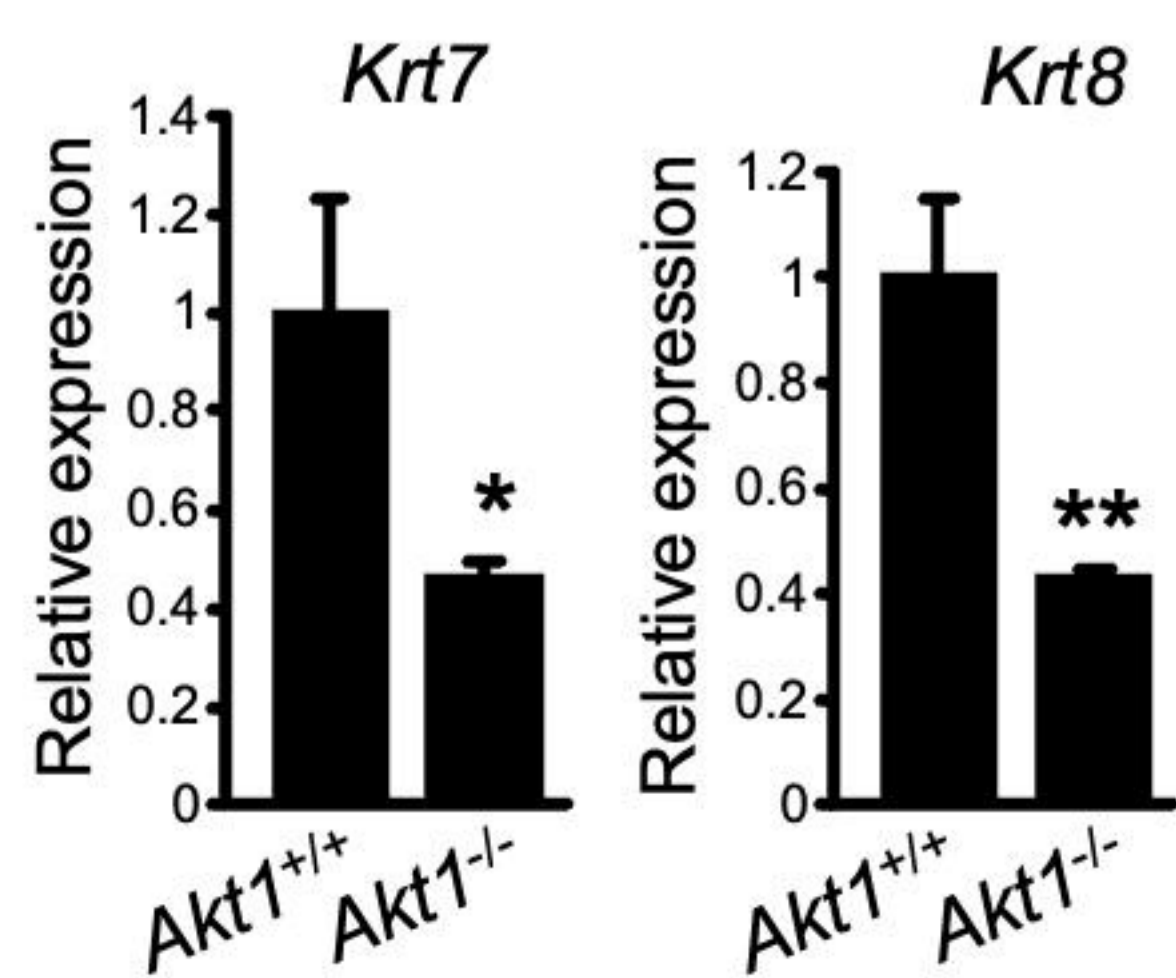


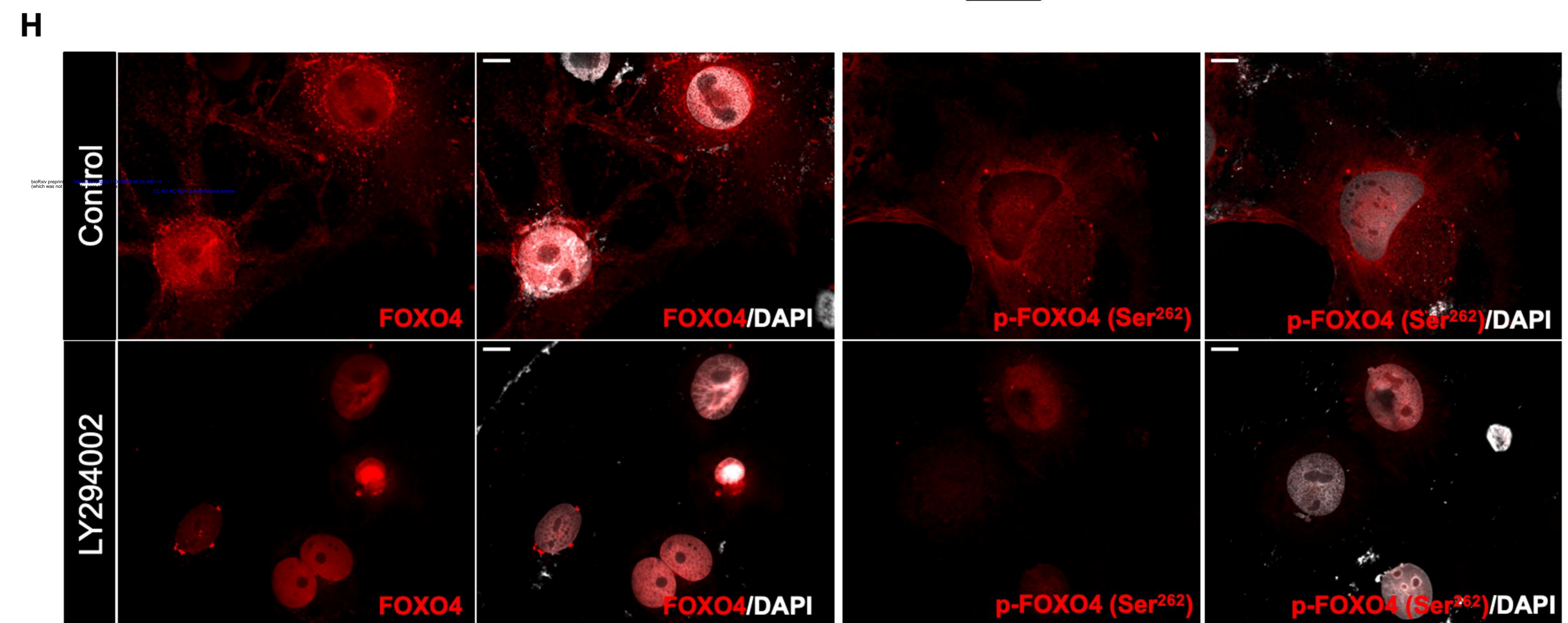
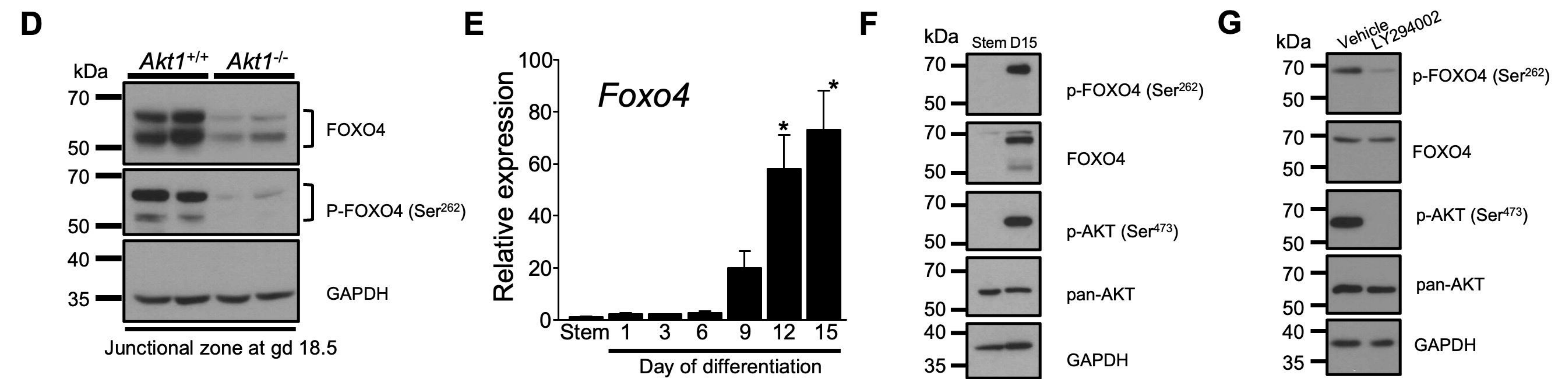
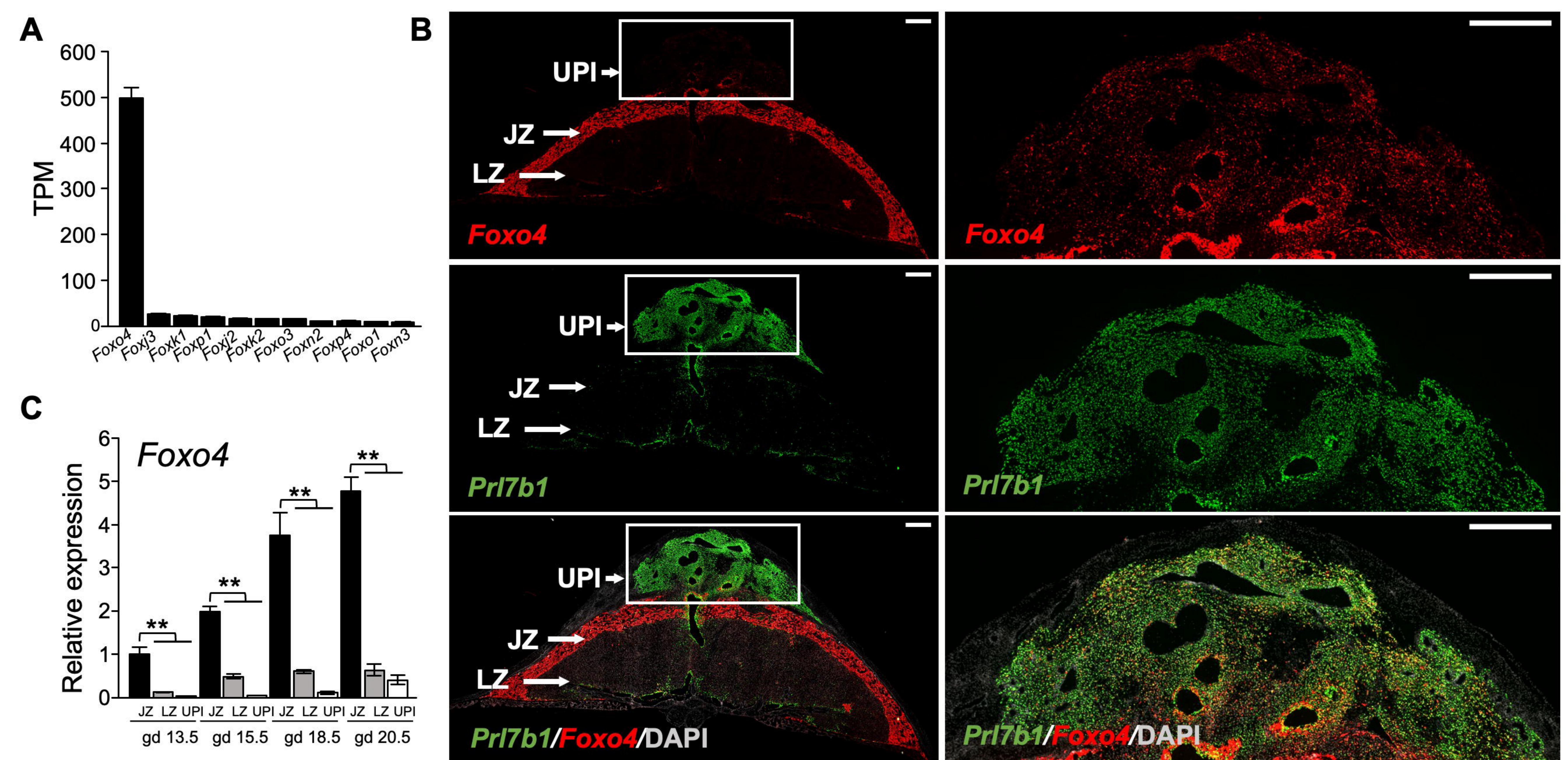
PH domain
 Kinase domain
 Regulatory region

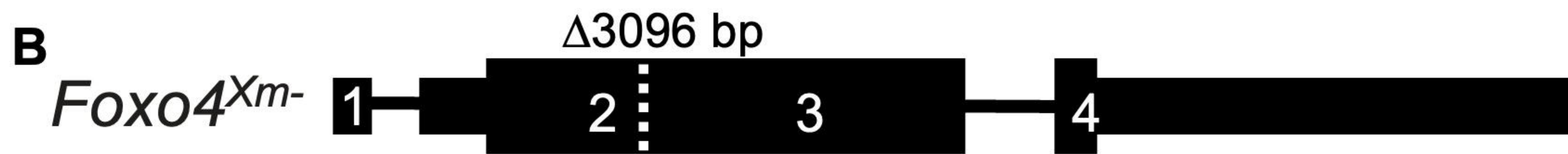
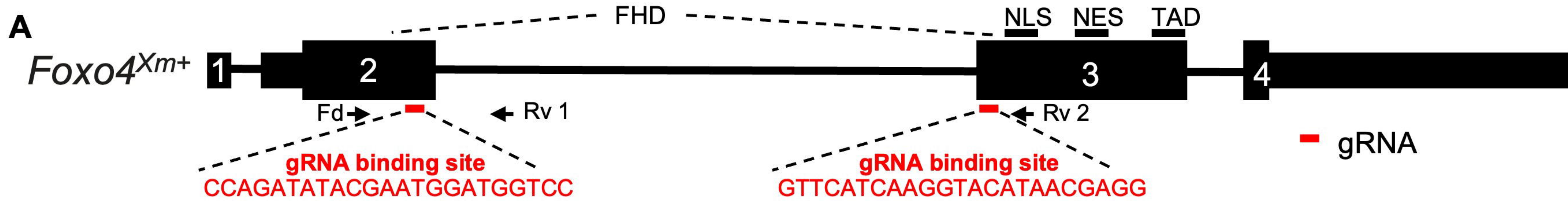
E





A*Akt1*^{+/+}*Akt1*^{-/-}**B****C****D****E****F**





C

FOXO4^{Xm+}

MEPENKKSATEAAAIIDLPDFEPQSRPRSCWPLPRPELATE
 PPEPSEVEPSLGQKVPTTEGHSEPTLLPSRLPEPAGGPQPEILG
 AVTGPRKGGSR**RNAWGNQSYAELISQAIESAPEKRLTLAQIYE**
WMVRTVPYFKDKGDSNSSAGWKNSIRHNL SLHSKFIKVHNEA
TGKSSWWMLNPDGGKGGKAPRRRAASMDSSSKLLRGRSKG
PKKKPSVLPAPPEGATPRSPLGHFAKWSSSPCPRNREEADV
 WTTFRPRSSSNASTVSTRLSMPRPESEVLAEEMPASASSYA
 GGVPTLSE**EDLELLDGLNL**ASPHSLLSRNLSSFSLQHPGLAG
 PLHSYGASLFGPIDGSL SAGEGCFSSSQSLEALLTSDTPPPPA
 DVLMTQVDPILSQAPTLLLLGGMPSSSKLATGVSLCPTPLEGP
 GPSNLVPTLSVMAPPPVMPGAPIPKVLGTPVLASPTEDFSHDR
MPQDLDLDMYMENLECDMDNIISDLMDGEGLDNFEPDP

FOXO4^{Xm-}

MEPENKKSATEAAAIIDLPDFEPQSRPRSCWPLPRPELATE
 PPEPSEVEPSLGQKVPTTEGHSEPTLLPSRLPEPAGGPQPEILG
 AVTGPRKGGSR**RNAWGNQSYAELISQAIESAPEKRLTLAQ****RP**
PARALGGC

D



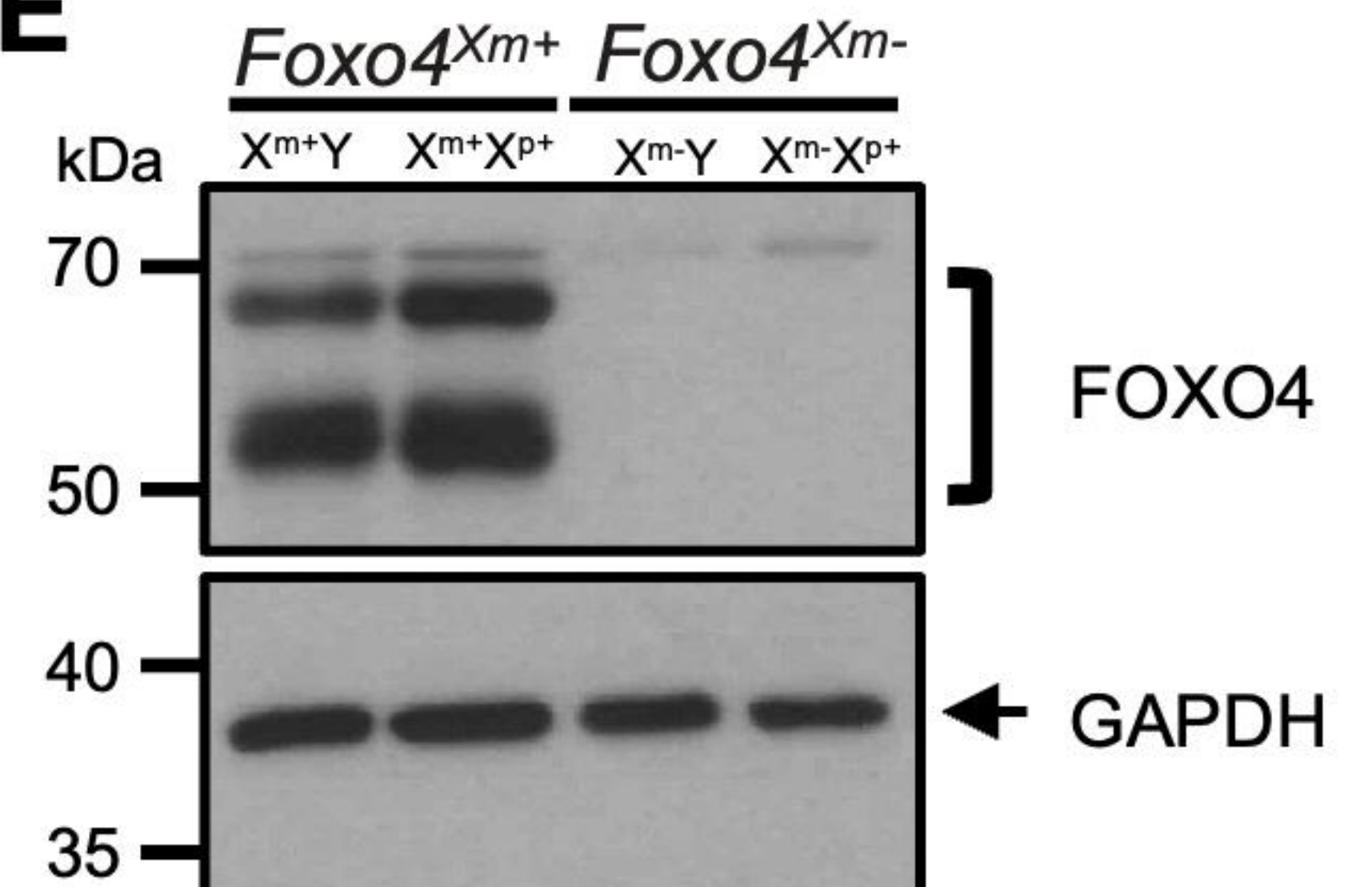
FHD

NLS

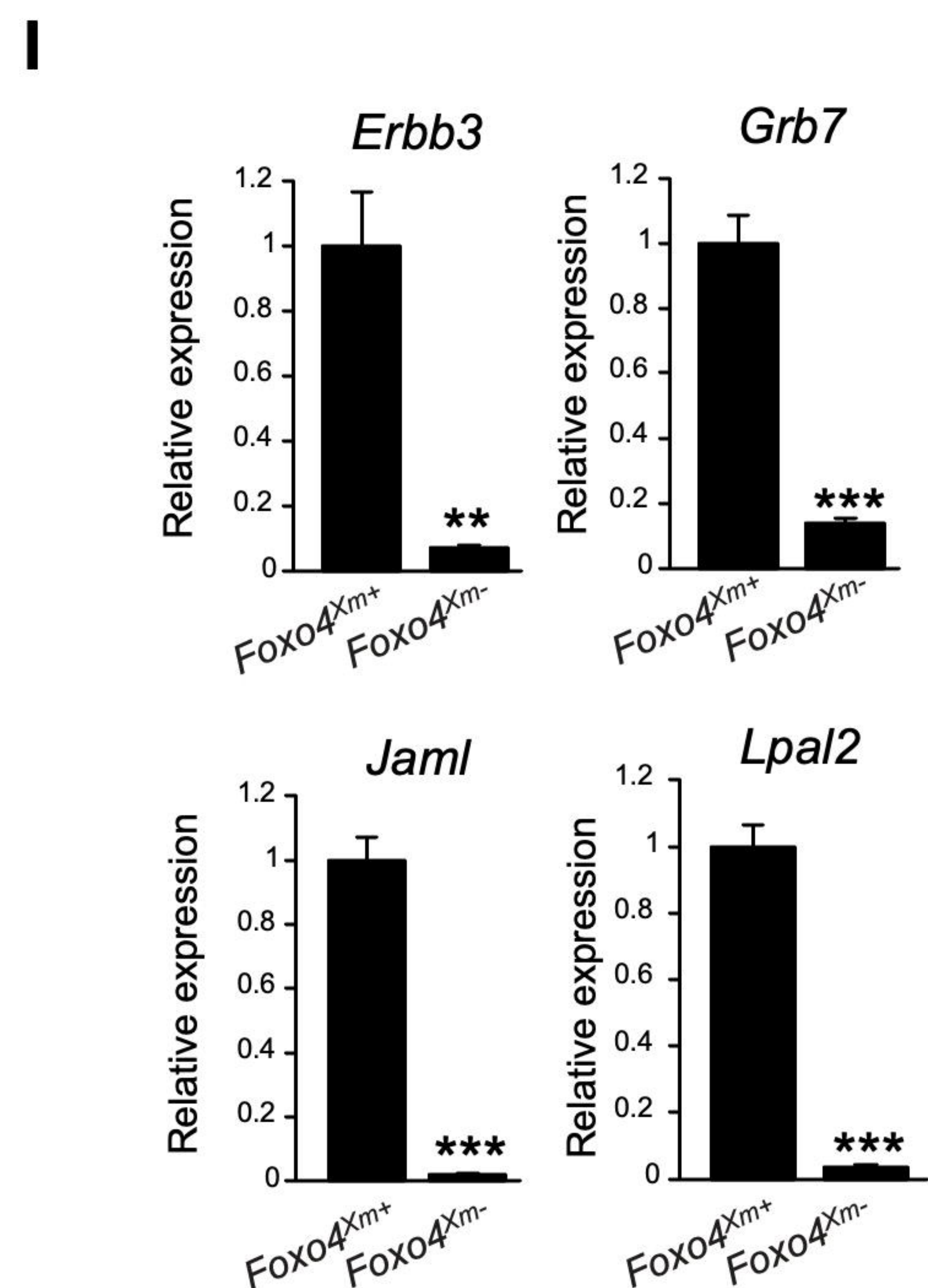
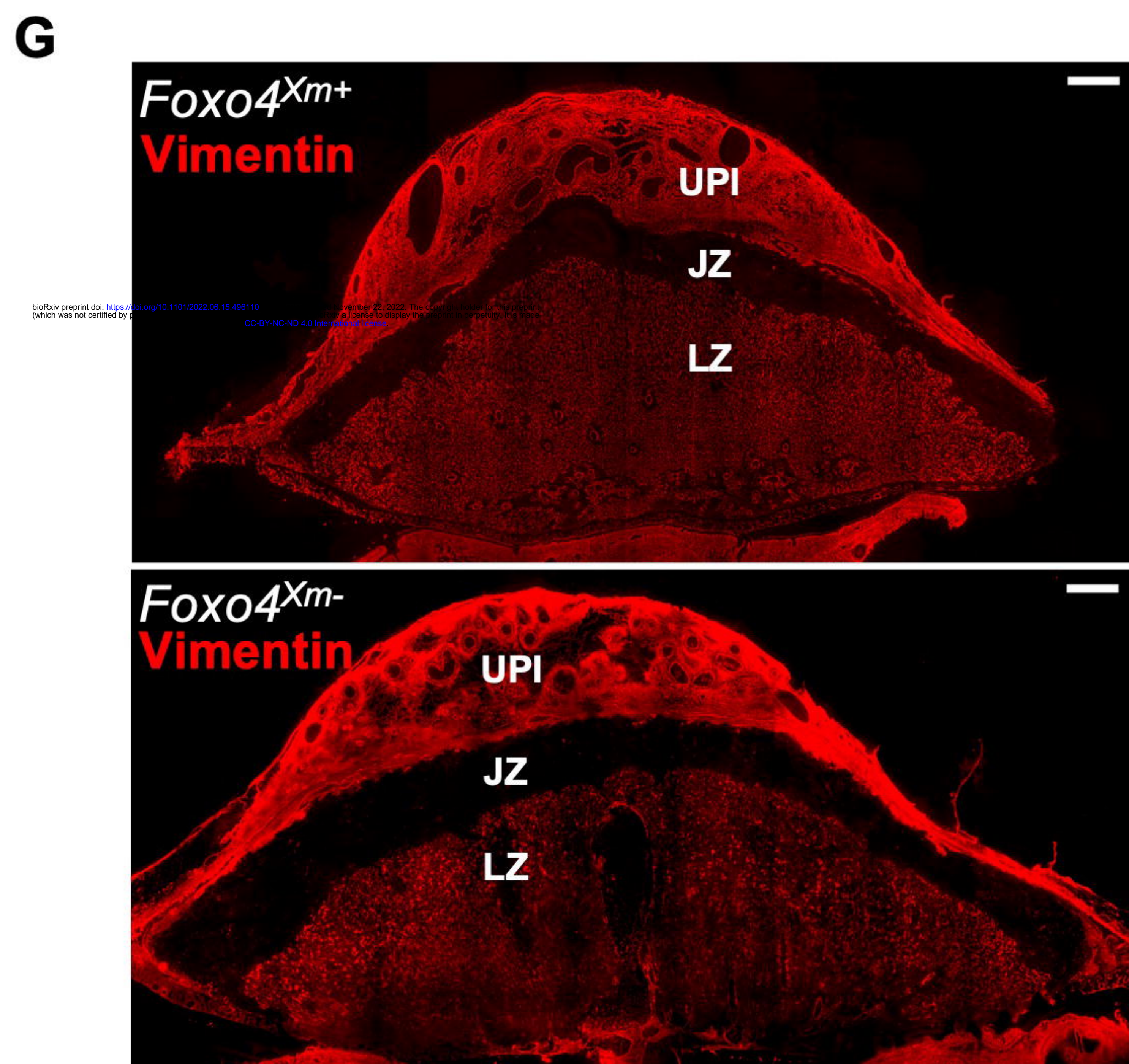
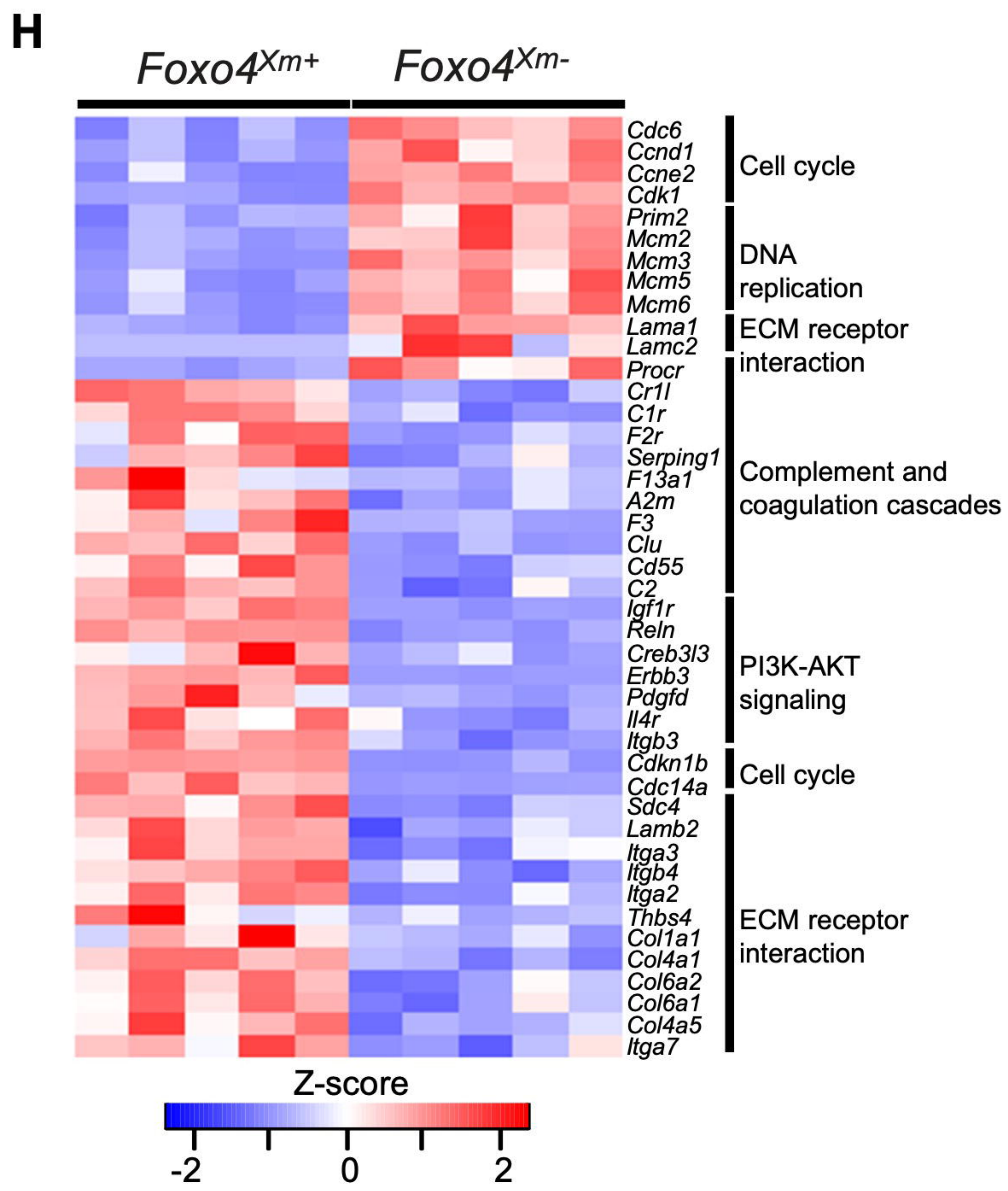
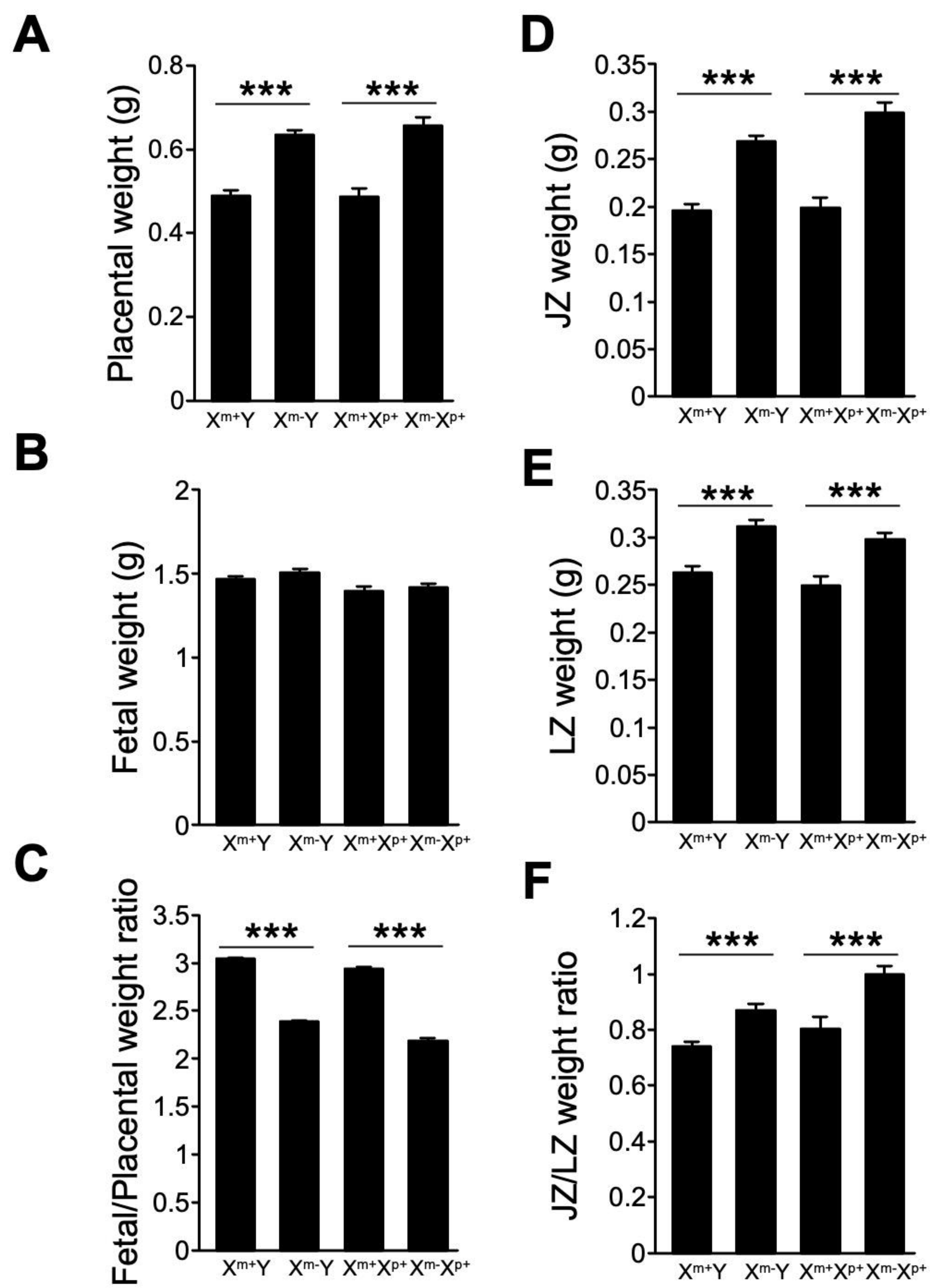
NES

TAD

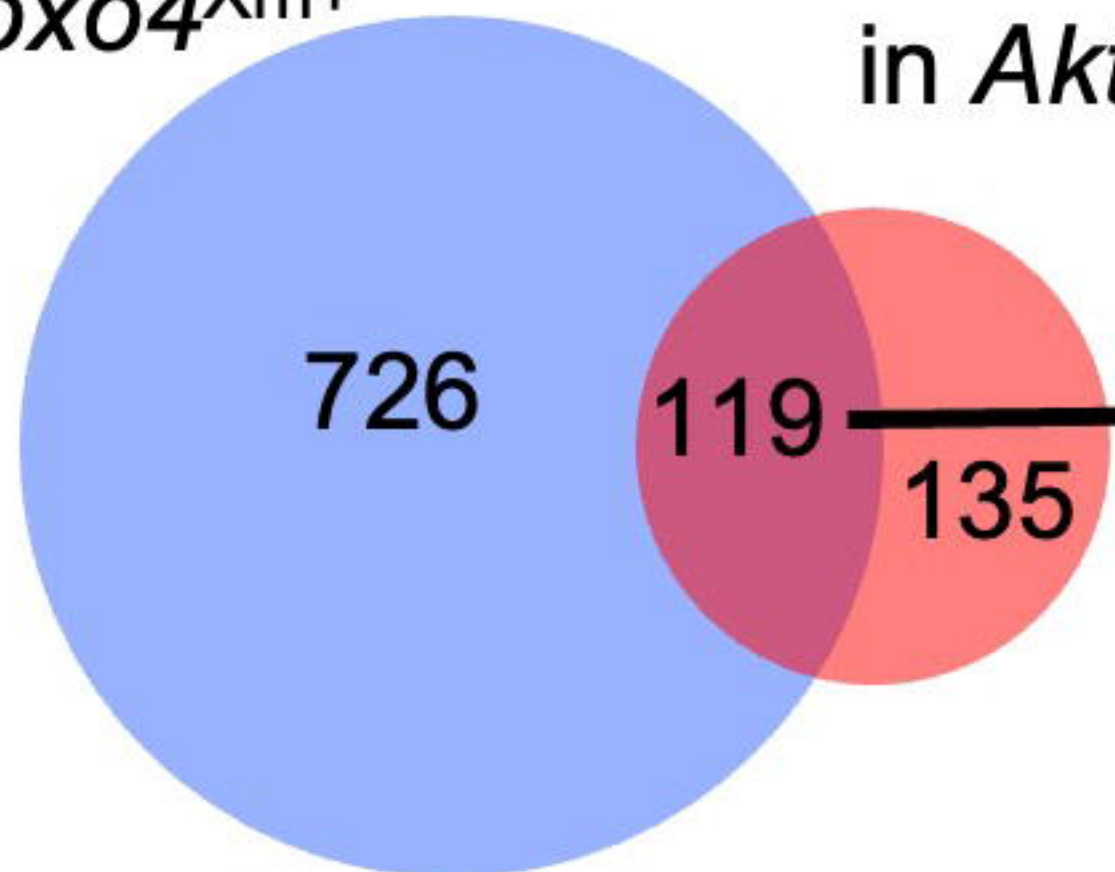
E



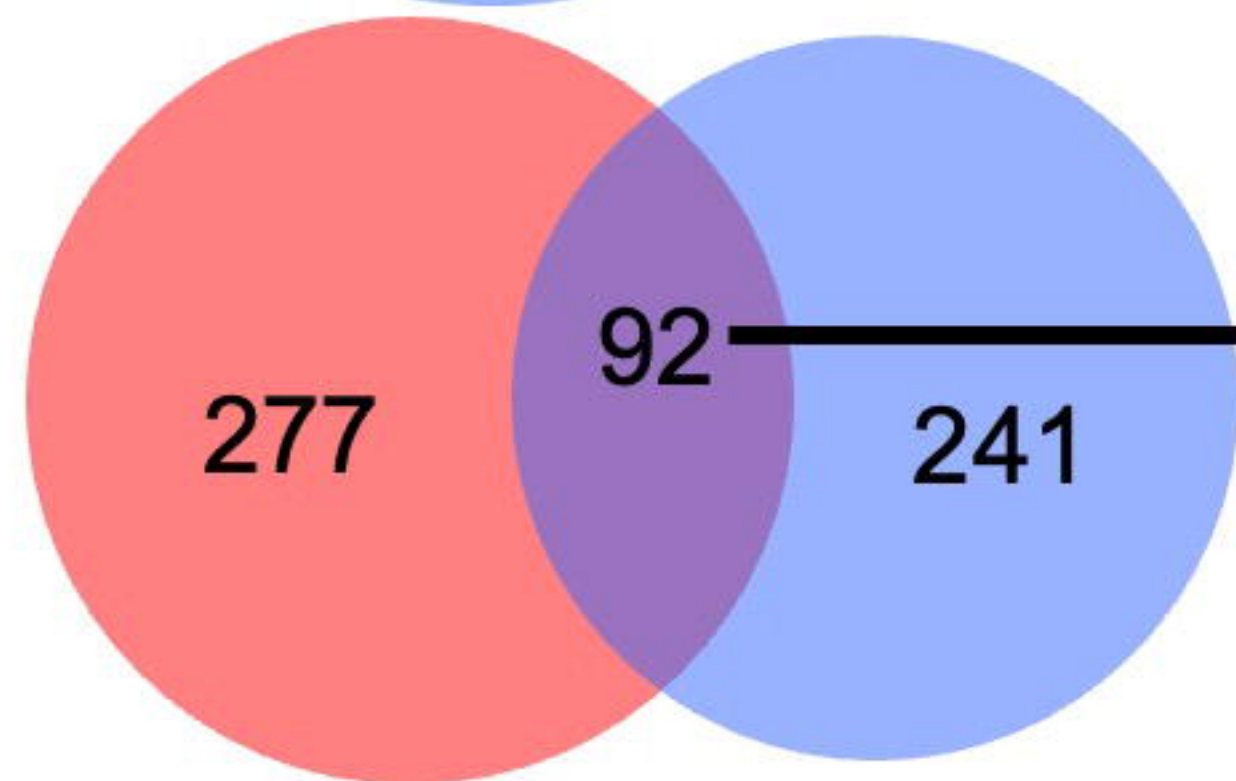
Junctional zone at gd 18.5



Genes downregulated
in $Foxo4^{Xm-}$ vs $Foxo4^{Xm+}$

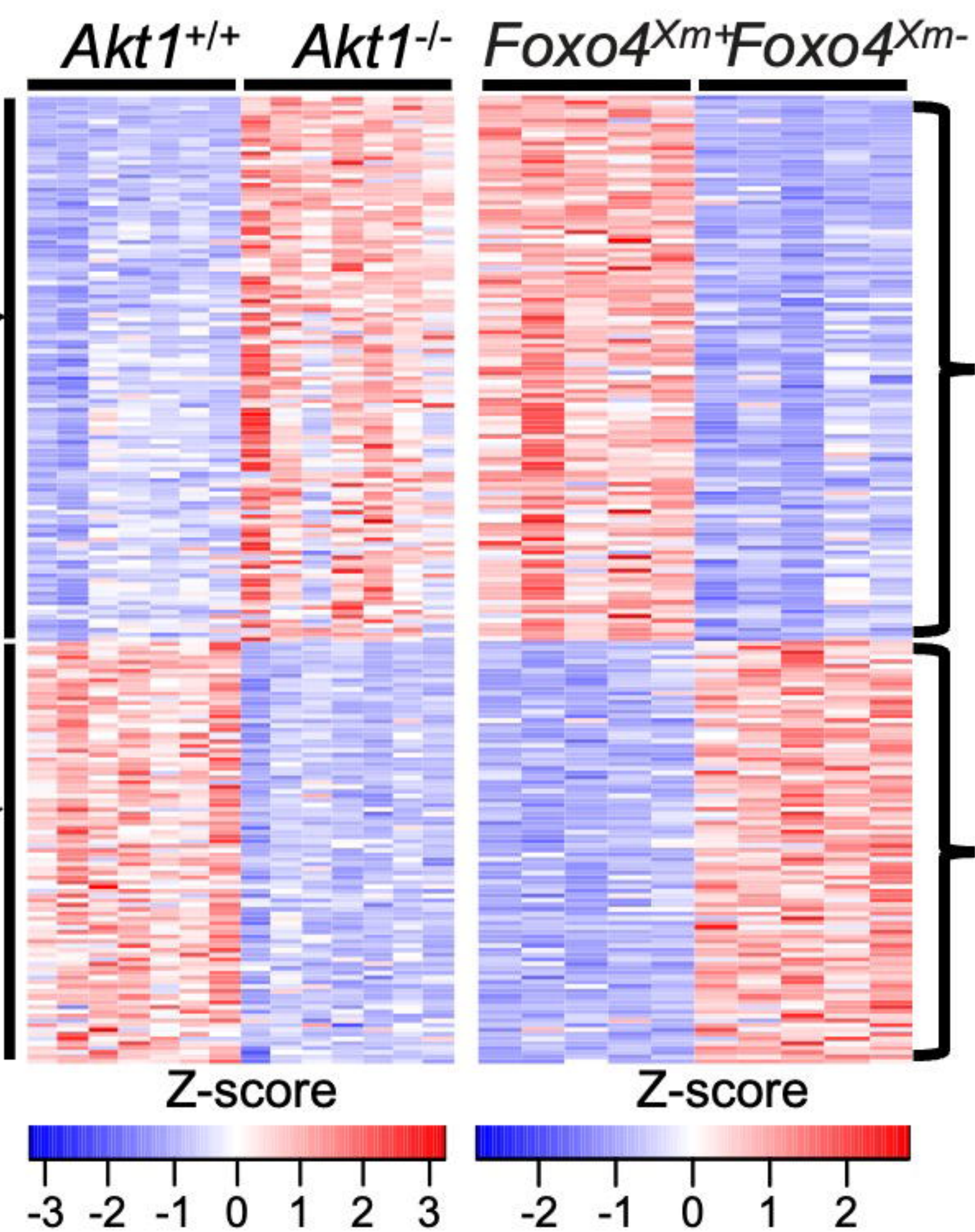


Genes upregulated
in $Akt1^{-/-}$ vs $Akt1^{+/+}$



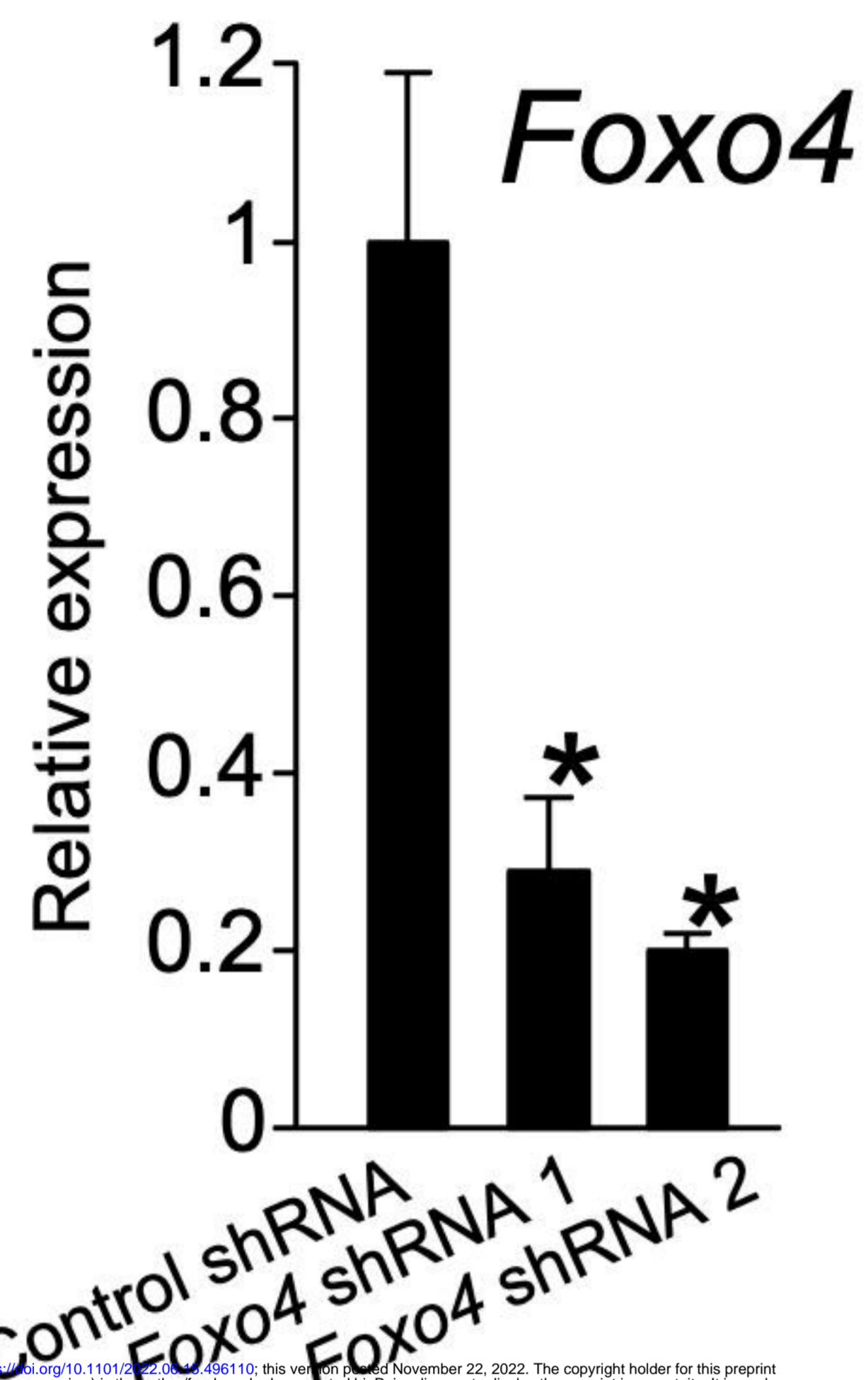
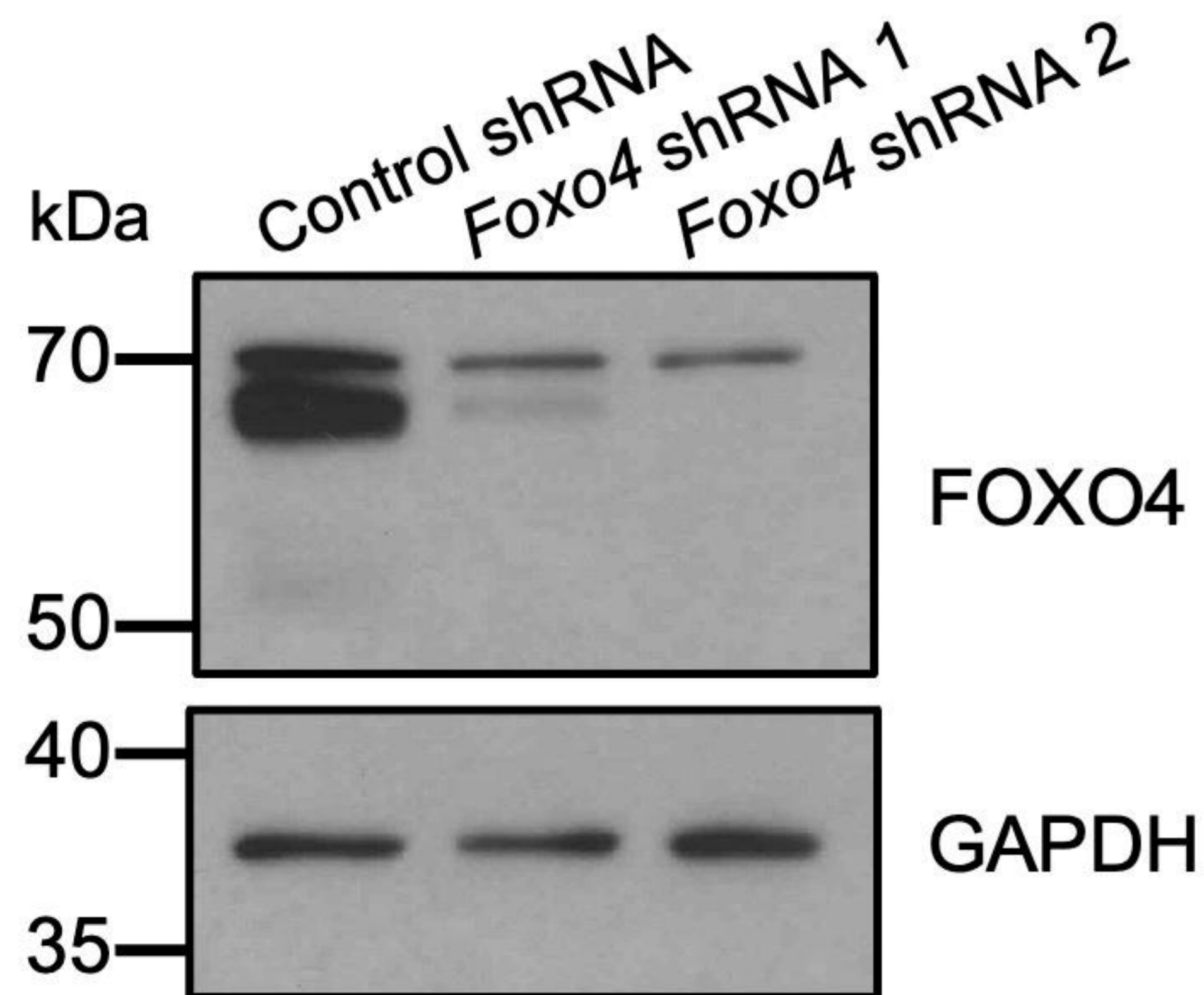
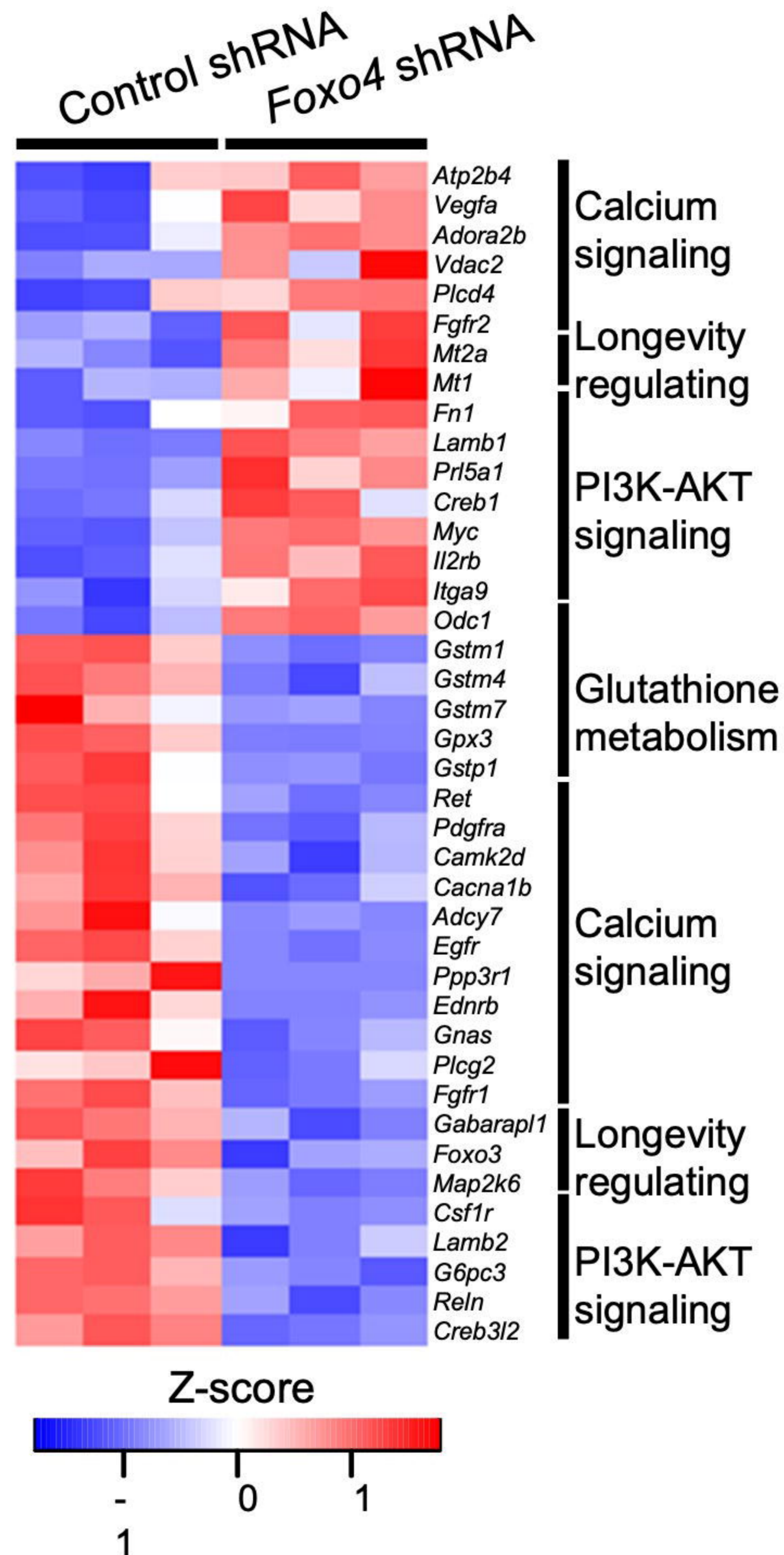
Genes upregulated
in $Foxo4^{Xm-}$ vs $Foxo4^{Xm+}$

Genes downregulated
in $Akt1^{-/-}$ vs $Akt1^{+/+}$



Upregulated in $Akt1^{-/-}$ vs $Akt1^{+/+}$
and
Downregulated in $Foxo4^{Xm-}$ vs $Foxo4^{Xm+}$

Downregulated in $Akt1^{-/-}$ vs $Akt1^{+/+}$
and
Upregulated in $Foxo4^{Xm-}$ vs $Foxo4^{Xm+}$

A**B****C****D**